KINEMATIC MODELS OF DEFORMATION IN SOUTHERN CALIFORNIA CONSTRAINED BY GEOLOGIC AND GEODETIC DATA

by

Lori A. Eich

S.B. Earth, Atmospheric, and Planetary Sciences
Massachusetts Institute of Technology, 2003

SUBMITTED TO THE DEPARTMENT OF EARTH, ATMOSPHERIC, AND PLANETARY SCIENCES
IN PARTIAL FULFILLMENT OF THE REQUIREMENTS FOR THE DEGREE OF

MASTER OF SCIENCE
AT THE
MASSACHUSETTS INSTITUTE OF TECHNOLOGY

FEBRUARY 2006

Signature of Author: .....
Department of Earth, Atmospheric, and Planetary Sciences
September 21, 2005

Certified by: .....
Bradford H. Hager
Cecil and Ida Green Professor of Earth Sciences
Thesis Supervisor

Accepted by: .....
Maria T. Zuber
E. A. Griswold Professor of Geophysics
Head, Department of Earth, Atmospheric, and Planetary Sciences

Kinematic Models of Deformation in Southern California Constrained by Geologic and Geodetic Data

by

Lori A. Eich

Submitted to the Department of Earth, Atmospheric, and Planetary Sciences
on January 20, 2006, in partial fulfillment of the
requirements for the degree of Master of Science in
Earth, Atmospheric, and Planetary Sciences

Abstract

Using a standardized fault geometry based on the Community Block Model, we create two analytic block models of the southern California fault system. We constrain one model with only geodetic data. In the other, we assign *a priori* slip rates to the San Andreas, Garlock, Helendale, Newport-Inglewood, Owens Valley, Sierra Madre, and Chino faults to create a joint geologic and geodetic model, using the *a priori* slip rates to refine the results in areas with limited geodetic data.

Our results for the San Andreas fault are consistent with geologic slip rates in the north and south, but across the Big Bend area we find its slip rates to be slower than geologic rates. Our geodetic model shows right lateral slip rates of 19.8 ± 1.3 mm/yr in the Mojave area and 17.3 ± 1.6 mm/yr near the Imperial fault; the San Gorgonio Pass area displays a left lateral slip rate of 1.8 ± 1.7 mm/yr. Our joint geologic and geodetic model results include right lateral slip rates of 18.6 ± 1.2 mm/yr in the Mojave area, 22.1 ± 1.6 mm/yr near the Imperial fault, and 9.5 ± 1.4 mm/yr in the San Gorgonio Pass area.

Both models show high values (10-13 ± 1 mm/yr) of right lateral slip to the east of the Blackwater fault along the Goldstone, Calico, and Hidalgo faults. We show that substantially different block geometries in the Mojave can produce statistically similar model results due to sparse geodetic data.

Thesis supervisor: Bradford H. Hager
Title: Cecil and Ida Green Professor of Earth Science

Acknowledgments

I would like to thank Brad Hager for all of his help on this project during the past 2 years. His patience and brilliance are a fantastic combination in a thesis advisor, and I could not have finished without him. I would also like to thank Brendan Meade for teaching me the nuances of his software and for responding to my countless emails, as well as John Shaw and Andreas Plesch for their help in importing the Community Block Model fault segments. I admire and thank Carol Sprague for her administrative help and patience throughout my attempts to graduate.

I would like to thank the National Aeronautics and Space Administration and the Massachusetts Institute of Technology for financial support.

Dr. Javier Santillan has great taste in audiobooks, and I acknowledge and appreciate that he shared them with me. I would like to thank Terri Macloon, Eric Hetland, Tom Herring, Simon McClusky, Philippe Vernant, Bob King, and Alison Cohen for their friendly smiles and passing conversations while at work.

I would like to acknowledge that JJ Lueck is a fantastic human being and the best support group I could ever ask for. I appreciate JJ's tolerance and calm attitude as well as his kitchen skillz. I also would like to thank MC Scat Cat for being my personal alarm clock every day this year.

Table of Contents

1. Introduction

Tectonic activity in southern California has been dominated by the San Andreas fault (SAF) for approximately the past 30 My (Atwater, 1970). To the northwest, near the Carrizo Plain and Cholame Hills in central California, the majority (~70 %) of the ~50 mm/yr relative motion between the Pacific and North America plates is accommodated by right lateral strike slip movement along the SAF (Sieh & Jahns, 1984). However, further south, the trend of the SAF changes from a strike of approximately 320° to 290° for 160 km (Figure 1), and a portion of the Pacific-North America relative motion is distributed throughout southern California along a complex network of auxiliary faults. In the Eastern California Shear Zone, *e.g.*, these faults are thought to accommodate 6-12 mm/yr (9-23%) of relative motion between the Pacific and North American plates (Dokka and Travis, 1990b).

To better understand the relationships among all of the faults across southern California, we imported the CBM and CFM fault traces (Plesch and Shaw, 2004) into the *blocks_sp1* program developed by Meade and Hager (2005) to create a kinematic block model of the area. We have further constrained the block model by including several *a priori* geologic slip rates along selected faults. Our results give estimates for many slip rates throughout southern California and can be used to estimate seismic hazard in the area.

Other block models have been applied to southern California tectonics in the past. Bird and Rosenstock (1984) used a planar geometry and hand-fit (rather than inverted) the model with respect to geologic data. Cheng *et al.* (1987) created a 12-block model using Bird and Rosenstock's geologic data as well as USGS trilateration data, resulting in a slip rate estimate of 20 mm/yr (lower than most previous estimates) as well as 6 mm/yr of crustal shortening across the SAF in the Transverse Ranges.

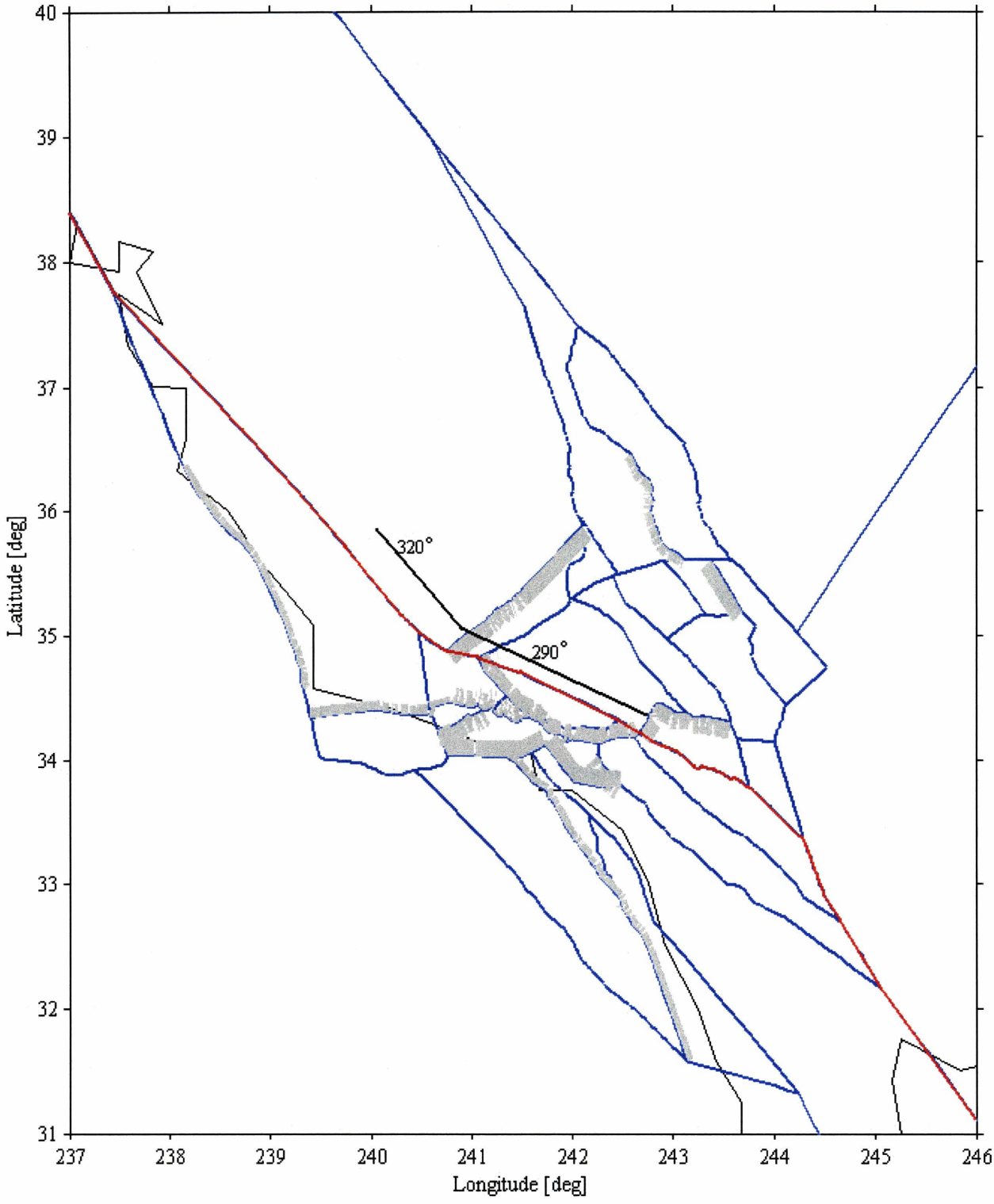

Figure 1: General view of our model in southern California, highlighting the San Andreas fault (SAF) in red. The solid black lines in the center of the image indicate the general trend of the surface trace of the SAF and the change in fault orientation at the latitude of the Mojave area.

Bird and Kong (1994) created a thin plate finite element model using the NUVEL-1 plate model and tested its estimates against geologic slip rates, principal stress directions, and trilateration and VLBI data. Souter (1998) inverted geologic slip rate estimates, then used a forward model to compare the estimates with geodetic data. This model was expanded upon by Meade and Hager (2005) who adapted Souter's work into an inverse model to calculate slip rate estimate from geodetic data.

Because we have used the same software as Meade and Hager (2005) to create our model, comparing the results of the two models can provide some insight into the strengths and weaknesses of *blocks_spl*. The program uses a weighted least squares inversion of a closed, spherical block geometry and a velocity field to estimate block rotations around Euler poles and to calculate slip rates along the block boundaries. The inversion can be further constrained by assigning an *a priori* slip rate to any fault.

Viscoelastic effects in the model are accommodated by locking depth and slip rate. In general, a deeper locking depth will incorporate strain from a greater distance (Meade and Hager, 2005). *Blocks_spl* calculates the elastic contribution to a velocity field. It assumes negligible coseismic strain release, and the geodetic velocity field represents the interseismic strain accumulation. The program first inverts the data into a set of rotation vectors by minimizing the sum of the weighted least squares, then uses the rotation vectors to create slip rate estimates along the faults. To reduce distortion, each fault is subdivided into segments such that no segment is longer than 10 km. Then, each small segment is locally projected onto a plane so that the fault trace is approximately equivalent to its great circle path. The elastic deformation is modeled within this projection, velocity contributions for each subsegment are combined, and the results are rotated back into the original orientation (east, north, up).

Meade and Hager apply *blocks_sp1* to create a purely geodetic kinematic model of deformation in southern California including 25 blocks bounded by 149 fault segments. The fault segments have an average length of 76.0 km. Each fault segment is assigned two endpoints, a dip, a locking depth, and a burial depth.

Our model differs from Meade and Hager's both in fault geometry and in geologic constraints. Faults are taken from the Community Block Model (CBM) and the Community Fault Model (CFM), and while similar in some respects to Meade and Hager's faults, they produce many different slip rate results when geodetically modeled with *blocks_sp1* using the same velocity data. Additionally, when our model is constrained by both geodetic and geologic constraints, it produces results that are more realistic than a purely geodetic model. The Community Block Model (CBM) replaced the fault geometries within the Mojave region of Meade and Hager's model. The main differences between the two models in this area are our division of Meade and Hager's Blackwater and Eastern Mojave blocks into the Blackwater, Calico, Avawatz, and Eastern Mojave blocks, as well as our locations of the Blackwater, Calico, Goldstone, and Avawatz faults.

The slip rates inferred from our model can provide useful data for seismic hazard analysis. Although the fault geometries in this model are much simpler than their real-world counterparts, they are specific enough to give realistic general estimates for slip rates along the faults. Additionally the model can be used to see the relationship between faults, *e.g.* an *a priori* slip rate can be assigned to a fault, which will in turn have an effect on the slip rate results for nearby faults.

2. Community Block and Fault Models

The primary region under consideration in the model is southern California, specifically the area bounded by (39N, 237E) and (31N, 246E) (Figure 1). Within this area, Plesch *et al.* (2004) have developed the Community Fault Model (CFM) as an effort toward a unified structural representation of the fault system in southern California (Figure 2). Additionally, Plesch *et al.* have created a Community Block Model (CBM) that uses the dominant faults of the CFM as guidelines to divide southern California into a series of adjacent tectonic blocks (Figure 3).

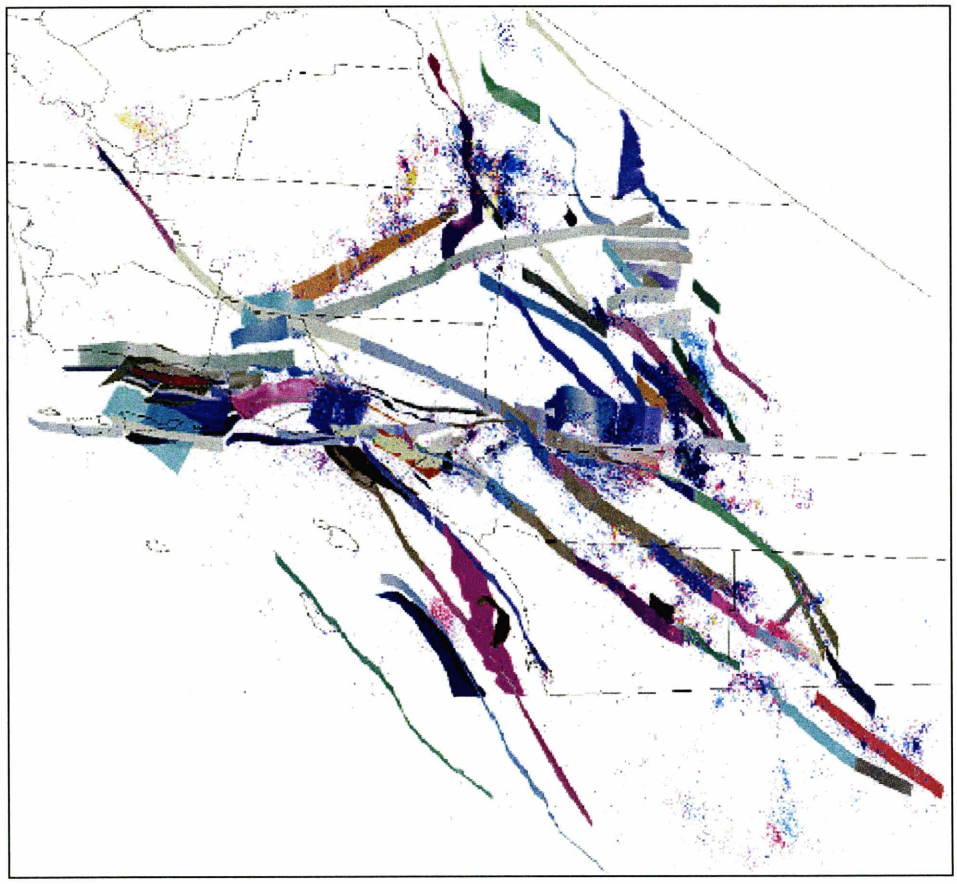

Figure 2: (From Plesch and Shaw, 2004) Perspective view of the SCEC Community Fault Model (CFM version 2). Seismicity is denoted by small colored points and is taken from Hauksson (2000).

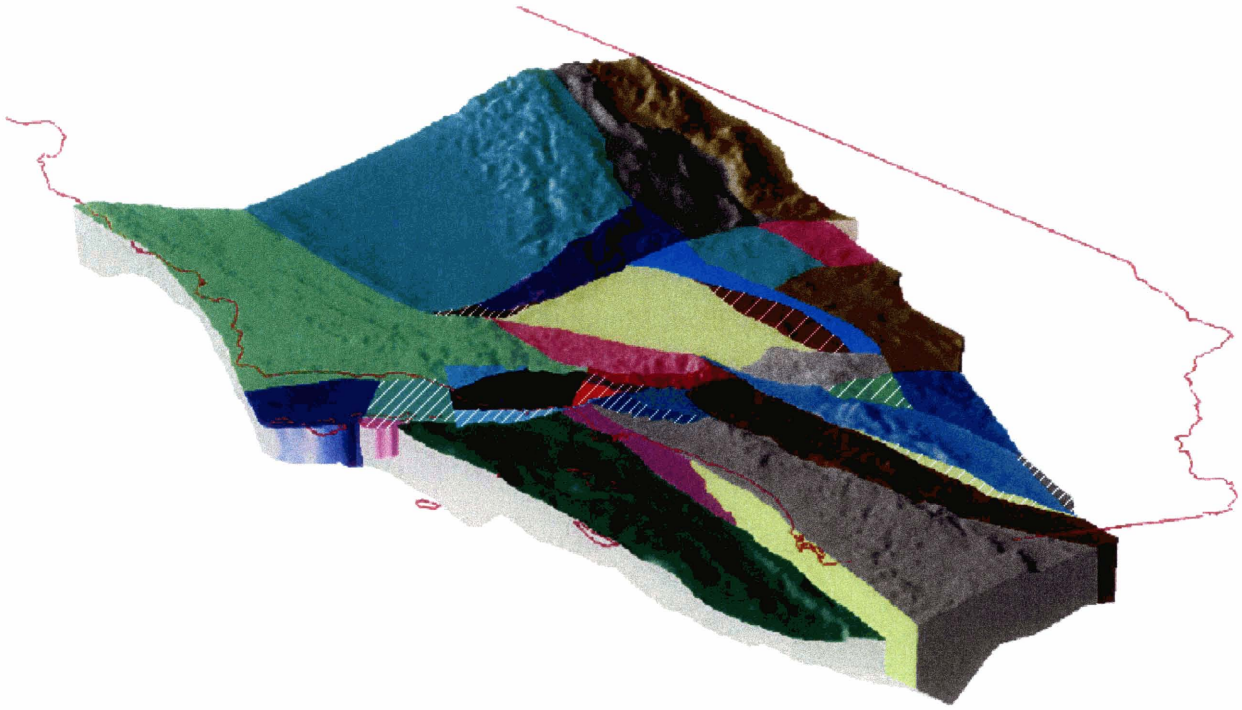

Figure 3: Adapted from the Community Block Model (Plesch and Shaw, 2004). North is oriented toward the top of the page. The 11 blocks with white stripes indicate blocks that exist in the CBM but have been merged with surrounding blocks in our model. Our model subdivides the lime green Coastal Ranges block in the northwest into 3 blocks; our model also contains an additional block to the east of the Avawatz and Ludlow faults in the Mojave area.

Figure 4 shows our model, derived from the CBM and containing 31 blocks: Avawatz (AW), Baja (BA), Big Pine (BP), Blackwater (BW), Calico (CA), Coastal Islands (CI), Coastal Ranges (CR), Death Valley (DV), Eastern Mojave (EM), Elsinore (EL), Helendale (HD), Little Lake (LL), Los Angeles (LA), Mojave (MJ), Nevada (NV), North America (NA), Oak Ridge (OR), Owens Valley (OV), Pacific (PA), Palos Verdes (PV), Pinto (PI), Salton Sea (SS), San Bernardino (SB), San Diego (SD), San Gabriel (SG), Santa Rosa (SR), Santa Susana (SU), Sierra Madre (SM), Sierra Nevada (SN), Ventura Basin (VB), and White Wolf (WW).

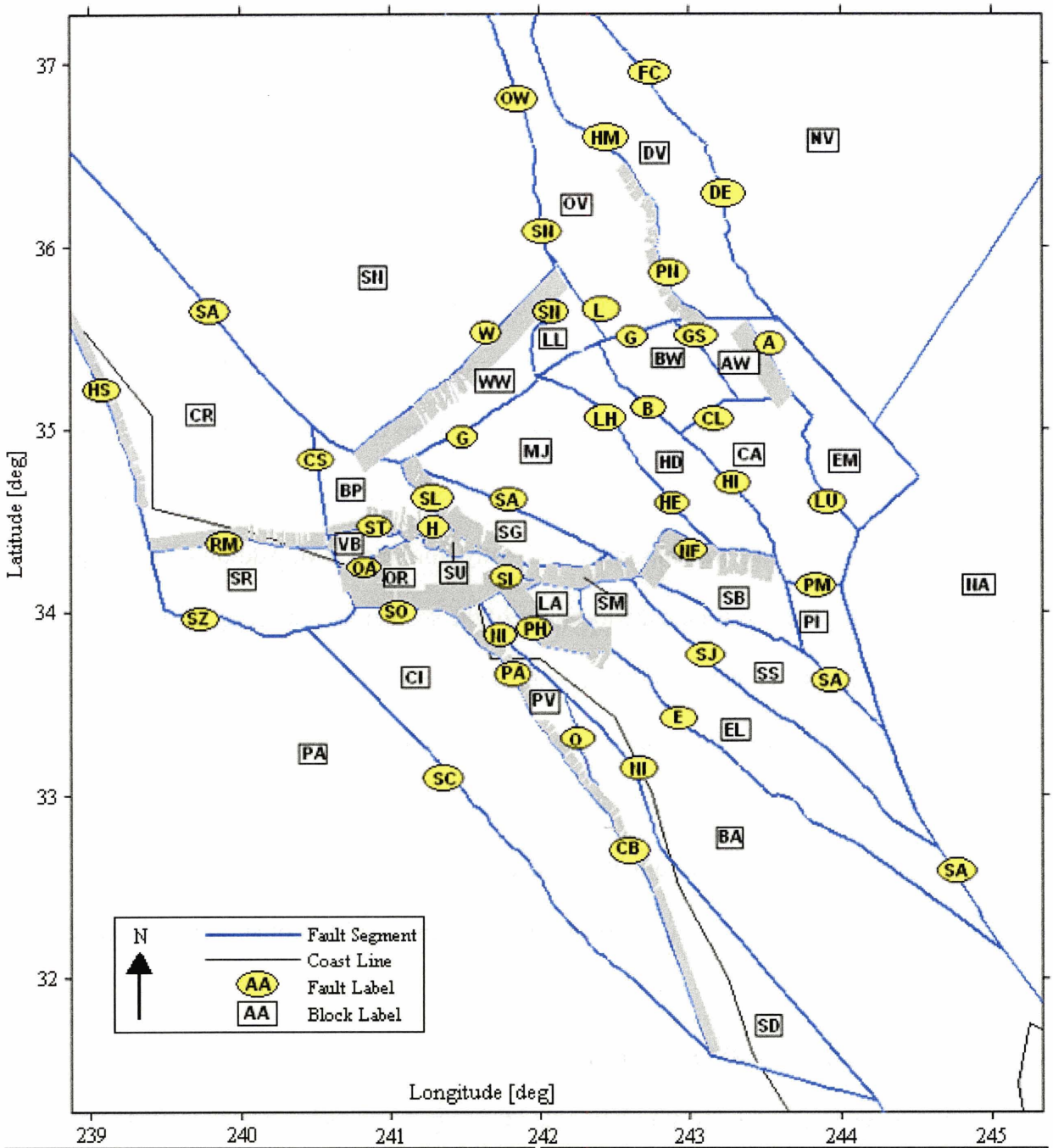

Fault Selection:		
A - Avawatz	HI - Hidalgo	PM - Pinto Mtn
B - Blackwater	HM - Hunter Mtn	PN - Panamint Vly
CB - Coronado Banks	HS - Hosgri-San Simeon	RM - Red Mtn
CL - Coyote Lake	L - Little Lake	SA - San Andreas
CS - Coastal Range	LU - Ludlow	SC - San Clemente
DE - Death Vly	LH - Lockhart	SI - Sierra Madre
E - Elsinore	NF - North Frontal	SJ - San Jacinto
FC - Furnace Creek	NI - Newport-Inglewood	SL - San Gabriel
G - Garlock	O - Oceanside	SN - Sierra Nevada
GS - Goldstone	OA - Oakridge	SO - Santa Monica
H - Holser	OW - Owens Vly	ST - San Cayetano
HE - Helendale	PA - Palos Verdes	SZ - Santa Rosa
	PH - Puente Hills	W - White Wolf

Block Selection:		
AW - Avawatz	LA - Los Angeles	SR - Santa Rosa
BA - Baja	MJ - Mojave	SU - Santa Susana
BP - Big Pine	NV - Nevada	SM - Sierra Madre
BW - Blackwater	NA - North America	SN - Sierra Nevada
CA - Calico	OR - Oakridge	VB - Ventura Basin
CI - Coastal Islands	OV - Owens Valley	WW - White Wolf
CR - Coastal Ranges	PA - Pacific	
DV - Death Valley	PV - Palos Verdes	
EM - Eastern Mojave	PI - Pinto	
EL - Elsinore	SS - Salton Sea	
HD - Helendale	SB - San Bernardino	
LL - Little Lake	SD - San Diego	
	SG - San Gabriel	

Figure 4: Fault and Block Selection. Faults are labeled in yellow ovals; blocks are labeled in white rectangles. The fault label legend is located in the lower left corner, and the block label legend is in the lower right corner. Fault segments are drawn in blue, and dipping faults have gray rectangles indicating dip direction. The Pacific coastline is shown in black. North is oriented toward the top of the page.

2.1 Fault Selection

Our fault selection is based on the CBM. Within the Mojave area (south of the Garlock fault and east of the SAF), we used segments imported directly from the CBM (Figure 5). Outside of the Mojave area, the CBM segment locations were unavailable. However, using visualization provided by the LA3D viewing tool (Southern California Earthquake Center, 2005) as well as the perspective view of the CBM (Figure 3), we were able to deduce the faults to use as boundaries for our blocks and import them directly from the CFM. Additionally, using these resources, we were able to estimate the locations of the segments connecting the CFM faults, creating a closed block geometry. Our fault segments average 14.0 km in length (before the segments are subdivided by *blocks_sp1*). The CFM faults are somewhat complicated and contain a series of many small fault segments (~3-4 km length), while the CBM faults are longer (~16-17 km) and more generalized. We used the CFM and CBM because they provide a control group (equivalent block geometries) to compare our results to the results of other modeling schemes.

2.2 Deviations from the CBM and CFM

Our model has slight deviations from the CBM geometries because the CBM contains several small blocks with limited velocity data. The perspective view of the SCEC CBM displays 36 tectonic blocks on the surface (over 75 blocks when including those that are located below the surface) of southern California using the CFM faults as guidelines for block boundaries. In areas where velocity data is sparse, we have merged blocks, reducing the number of southern California blocks to 27.

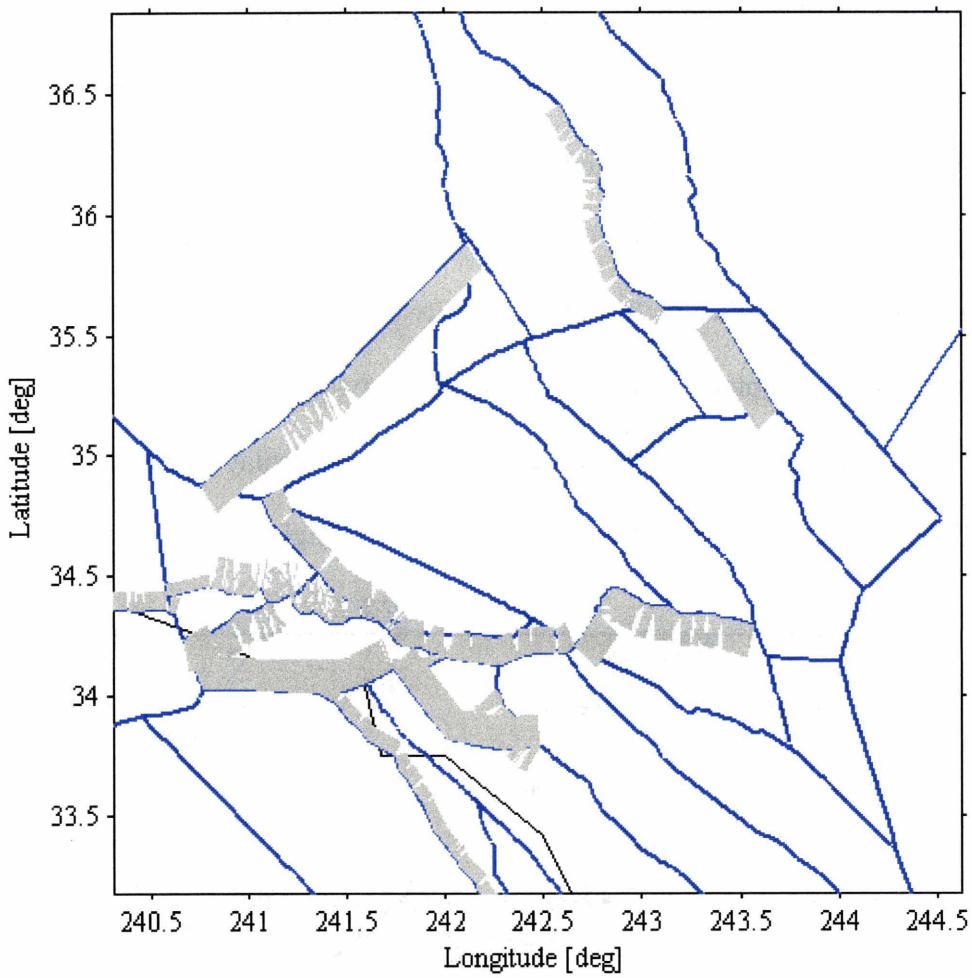

Figure 5: The Mojave area of our model. The fault segments in this area (shown in blue) are longer and more generalized than faults throughout the rest of southern California because they are taken from the CBM rather than the CFM (Plesch and Shaw, 2004). The selected block boundaries in the Mojave area are delineated by the San Andreas, Garlock, Helendale, Lockhart, North Frontal, Pinto, Hidalgo, Calico, Blackwater, Goldstone, Coyote Lake, Avawatz, and Ludlow faults. Dipping faults have gray rectangles in the direction of dip.

The block bounded by the Helendale and Lenwood faults (shown in maroon with white stripes in Figure 3) contained only one velocity station, and the resulting geodetic model showed the block moving northwest at a rate of ~4 ± 6 mm/yr with respect to the surrounding blocks (right laterally along the Lenwood fault and left laterally along the Helendale fault), as if the other blocks were squeezing it out of the way (Figure 6). We merged this block with its neighbor to the northeast to create a single block bounded by the Helendale, Lockhart, Garlock, Blackwater, Calico, Hidalgo, and East North Frontal faults. Similarly, the Pinto Mountain fault

was dividing our San Bernardino block, causing the northern portion to contain no velocity data points and the southern portion to contain very few. The resulting slip rates from a model containing both blocks showed a very high right lateral slip rate along the Pinto Mountain fault, with correspondingly high uncertainty. Unrealistic slip rates with high uncertainty are characteristic results of blocks with few or no velocity data points. We eliminated the Pinto Mountain fault within this block, effectively merging the two portions to create our San Bernardino block. The other blocks that have been combined displayed similar characteristics to the merged blocks in the Mojave and were dealt with accordingly.

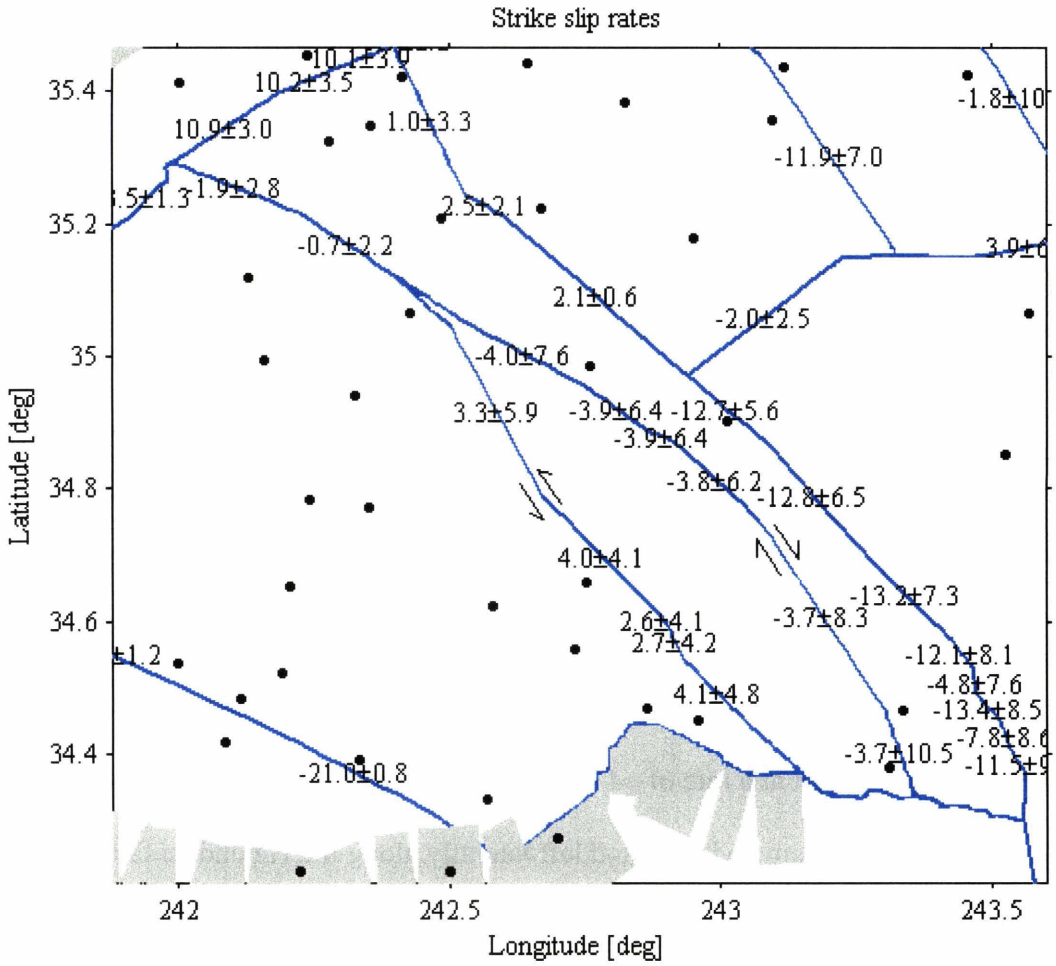

Figure 6: Strike slip results for a geodetic model that includes the block bounded by the Helendale and Lenwood faults, which contains only one velocity station (stations indicated by small black circles). In this model, the block is moving toward the northwest at approximately 4 mm/yr with very high uncertainty. The high uncertainty and unlikely behavior of the faults surrounding this block are characteristic model results for blocks with very few enclosed velocity stations.

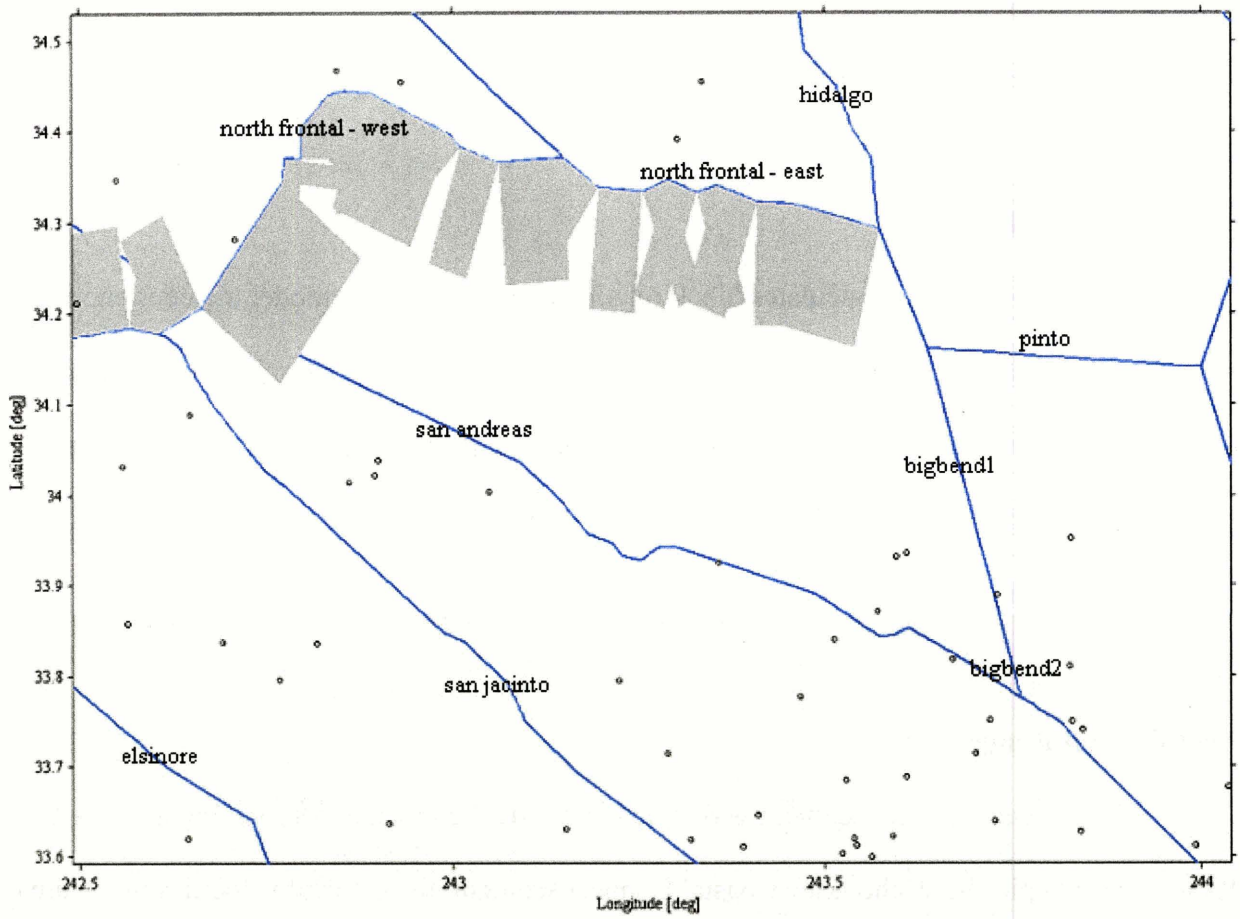

Figure 7: Our preferred model geometry in the San Bernardino Mountains area. The small circles indicate locations of velocity stations. The proximity of the stations near bigbend1 and bigbend2 lead to a more realistic slip rate (*i.e.* reduced left lateral motion) along the San Andreas fault, causing us to choose Meade and Hager's bigbend segments over Plesch and Shaw's Burnt Mountain segments.

One of the blocks with limited velocity data, the San Bernardino block (Figure 7), was found to produce a left-lateral slip rate along the SAF using a geodetic inversion model. Assuming the right lateral motion of the SAF to be the dominant tectonic factor in the southern California fault system, we chose to adopt a block geometry that would provide a close match to the CBM while maximizing the right lateral slip of the SAF – San Bernardino. We replaced the CFM Burnt Mountain fault with Meade and Hager's bigbend1 and bigbend2, which resulted in a reduction of the left lateral slip values for most of the SAF segments. The proximity of the velocity stations to the edge of the block was the primary factor in obtaining more reasonable results near this block. Given the small number of velocity stations available on this block, the

block geometry proved an important factor in the slip rate results; Meade and Hager's geometry produced the more favorable set of slip rates.

2.3 Additional blocks

Because *blocks_sp1* calculates block rotations on a sphere, our model includes enough blocks to encompass the entire earth. In addition to the 27 southern California blocks in our model, we have included four exterior blocks: Nevada, the Pacific plate, the North American plate, and the rest of the world. The 27 southern California blocks include two block divisions that are not included in the CBM.

2.3.1 Coastal Range

The Coastal Connect segment was added to divide the block encompassing the Coastal Range into two pieces. Without the Coastal Connect segment, the residual velocities in the area suggest that a structure may be missing from the model (Figure 8). Residual velocities in the Coastal Range block are high and can give some insight into the behavior of the block within the model. The southeast portion of the block appears to have residual vectors toward the south and southwest, while the residual velocities in the northwest portion are headed toward the north and northeast. The residual velocities within the block imply a clockwise rotation that is not accommodated by the model. If the Coastal Connect segment is included, the residual velocities become two sets of counterclockwise vectors, rather than one set of clockwise vectors.

Including the Coastal Connect segment reduces the X^2/DOF of the model by over 15%. Because the separation of these two blocks produces a statistically more accurate result than leaving them together, the model suggests that deformation may exist that is not expressed as a

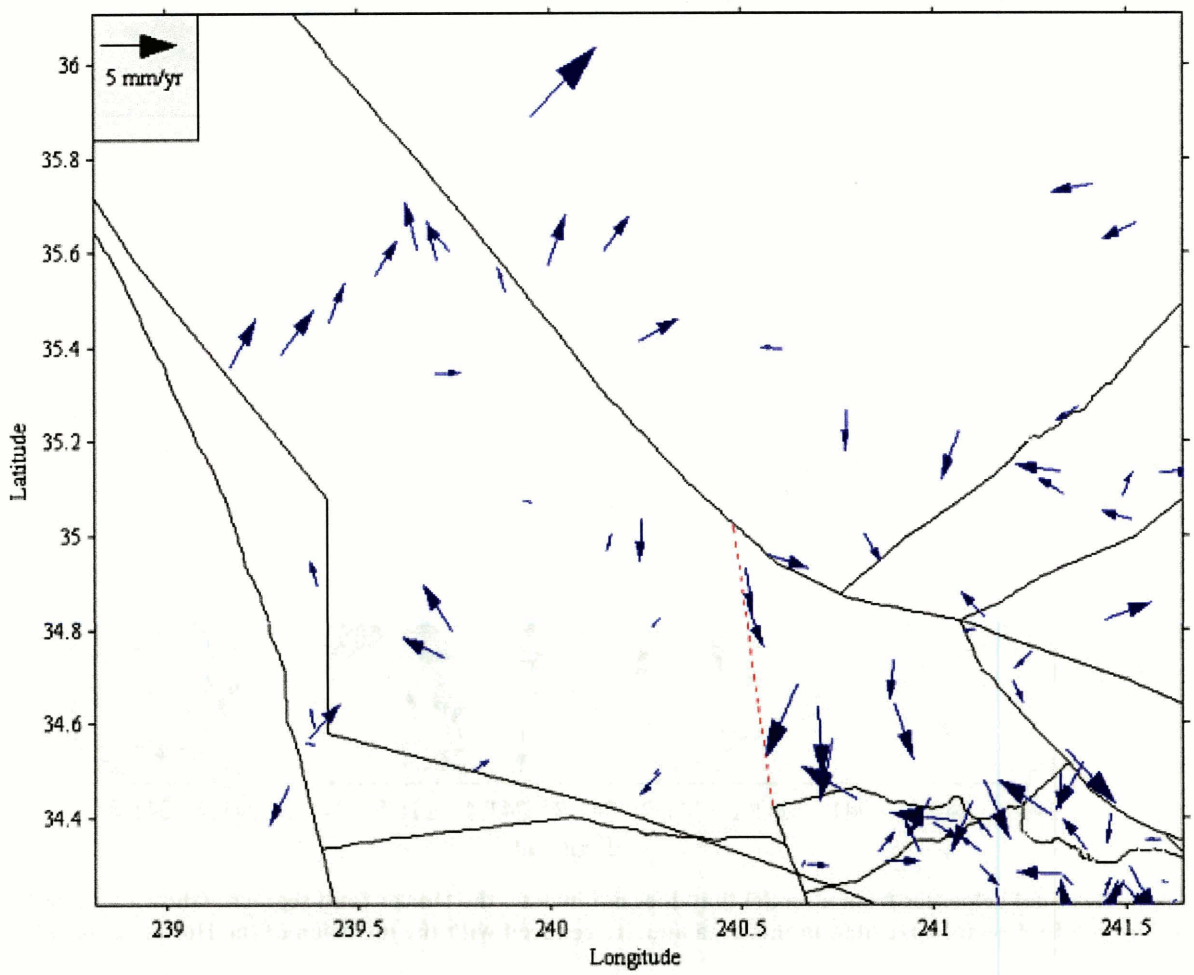

Figure 8: Residual velocities from a geodetic model which does not contain the Coastal Connect segment that separates the Coastal Range block from the Big Pine block. Our selected location of the Coastal Connect segment is indicated by the dashed red line.

discrete fault in this region. We have chosen an approximate location of the deformation using Meade and Hager's Coastal Range Connect segment as a guideline, but given that there is no local fault trace to use as an obvious block boundary, the deformation may be distributed more widely across the Coastal Range and Big Pine blocks than can be delimited by a simple block boundary.

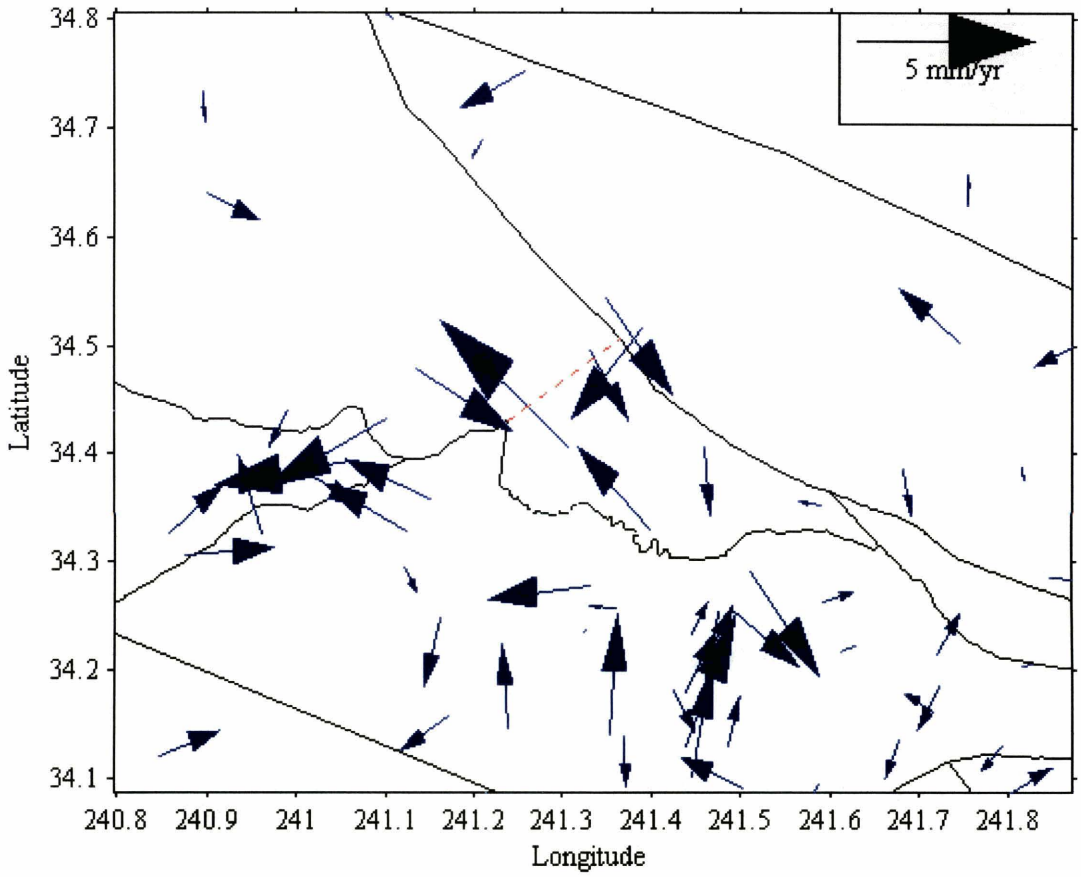

Figure 9: Residual velocities from a model that does not include the Holser fault segment (shown as a dashed line). The residual vectors are high in this area and are reduced with the inclusion of the Holser segment.

2.3.2 Holser Fault

In addition to the Coastal Connect division, the Coastal Range block was further divided with the Holser fault segment. Without the Holser segment, the residual velocities on either side of the presumed location of the Holser segment are apparently headed in opposite directions (Figure 9). Adding the Holser segment reduces the X^2/DOF of the model by over 2% and halves the local residual velocities.

2.3.3 Eastern Mojave

We have included an Eastern Mojave block to the east of the Avawatz and Ludlow faults. This block was included in earlier versions of the CBM and is present within the LA3D block model (Southern California Earthquake Center, 2004). We find that removing this block from our model increases our X^2/DOF and results in a normal sense of dip slip along the Avawatz fault, as well as left lateral motion along the Blackwater fault. The Eastern Mojave block provides a buffer zone between the intersection of the Mojave region, Nevada, and North America, and it improves the fit of our global block model.

3. Methodology

3.1 Geologic Slip Rates

Our goal was to determine if we could find a model that is consistent with both geodetic and paleoseismic data. To make the model conform to paleoseismic data, we imposed long-term geologic slip rates as additional *a priori* constraints to the geodetic inversion.

We selected slip rates for the Newport-Inglewood, San Andreas – Carrizo Plain, Garlock, Helendale, Owens Valley, Chino, and Sierra Madre fault zones (Table 1).

Fault	Slip Rate (mm/yr)	Source
Newport-Inglewood (north)	1.8 ± 0.5	Fischer & Mills (1991)
San Andreas – Carrizo Plain	33.9 ± 2.9	Sieh & Johns (1984)
Garlock	6.5 ± 2.5	McGill & Sieh (1991)
Helendale	0.8 ± 0.5	Dokka & Travis (1990a)
Owens Valley	2.0 ± 1.0	Wesnousky (1986)
Chino	0.4 ± 0.1	Walls & Gath (2001)
Sierra Madre	0.8 ± 0.4 (dip slip)	Walls (2001)

Table 1: Selected *a priori* slip rates for joint inversion of geologic and geodetic data. All slip rates refer to right lateral slip, with the exception of Garlock (left lateral) and Sierra Madre (thrust).

Our slip rates were taken from the Southern California Fault Activity Database (FAD) (Southern California Earthquake Center, 2003). Because many of our fault segments are small, we have chosen geologic slip rates that have been measured in the field at specific longitude-latitude coordinates to ensure that our *a priori* constraints have been assigned to the proper location. The high detail of our fault segments causes many of the segments to be oriented in a direction different from the general trend of the faults they represent; to reduce the error in assigning an *a priori* slip rate to a fault with an improper strike orientation, we prefer rates whose location coordinates correspond with specific fault segments in our model. Additionally, the slip rates are selected such that the constrained faults are distributed across a wide range of the map area. Of the rates in the FAD, our selected slip rates represent the subset that can fulfill these requirements.

We have also included geologic constraints for the SAF – San Gorgonio Pass and the North Frontal fault zone. The velocity data in the block located south of the North Frontal fault zone is very limited, leading to geodetic results that include left lateral strike slip rates along the SAF and very high rates of thrusting on the North Frontal fault zone (Figure 10). Slip rate measurements in this area are limited, although Harden and Matti (1989) used alluvial fan offsets to estimate a slip rate of 11-35 mm/yr, with a preferred rate of 21-31 mm/yr. The behavior of the SAF in this area is not well-known, but given the behavior of the rest of the fault, it is highly unlikely that the SAF is moving left laterally. To accommodate these factors, we gave the SAF – San Bernardino a loose geologic constraint of 10.0 ± 10.0 mm/yr right lateral slip, *i.e.* requiring the fault to have right lateral slip, but allowing it to vary to whatever value will fit the model. Additionally, we put a loose constraint of 3.0 ± 3.0 mm/yr on the thrusting rate of the North Frontal fault zone to ensure that it maintained a reasonably low slip rate. Constraining the SAF to

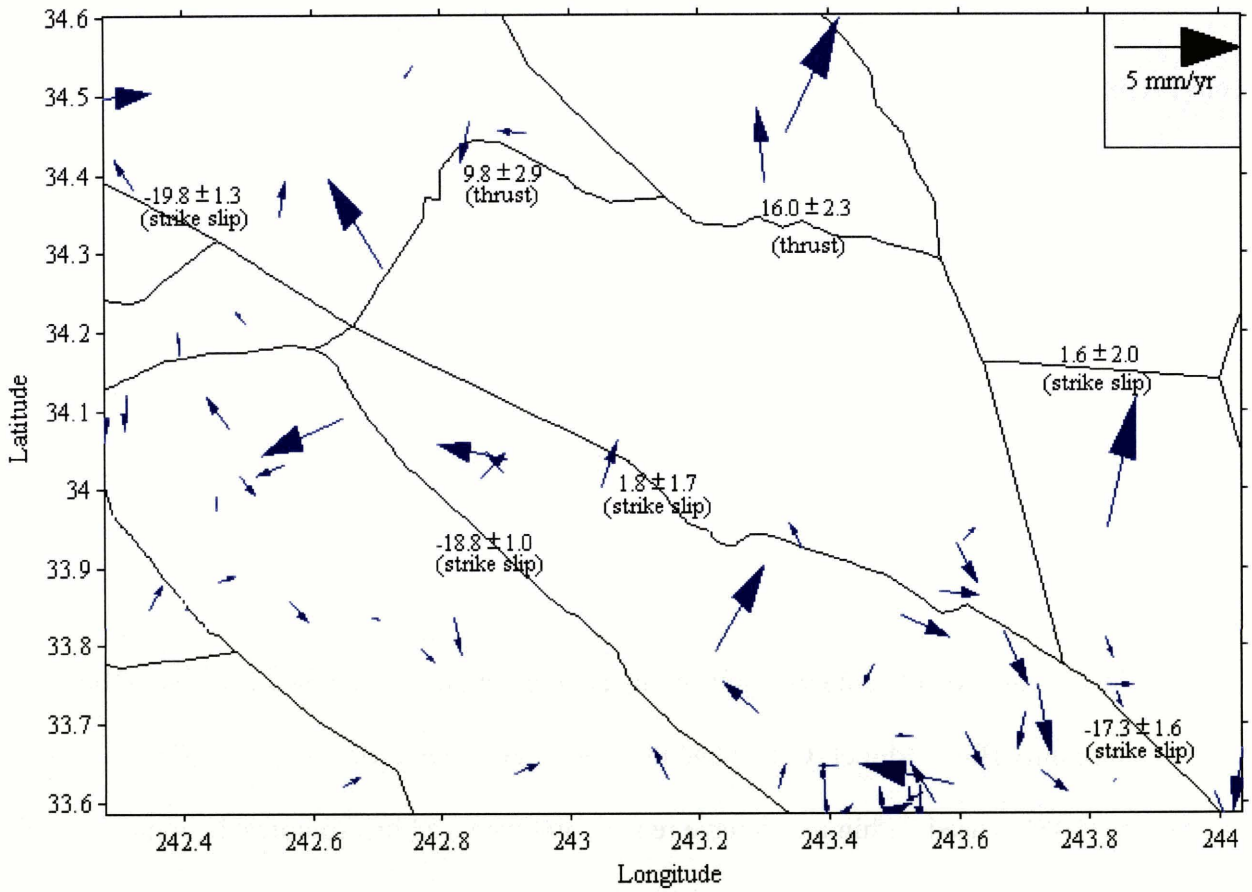

Figure 10: San Bernardino block with selected slip rates from our geodetic model, which includes the bigbend1 and bigbend2 segments from Meade and Hager (2005). For strike slip rates, negative values refer to right lateral slip and positive values to left lateral slip. The blue arrows are local residual velocities. The San Andreas fault moves left laterally along the southwest border of the San Bernardino block, with high thrust slip rates in the North Frontal fault zone as well as a high right lateral slip rate along the San Jacinto fault.

a higher right lateral slip rate or the North Frontal fault zone to a lower thrust rate causes statistical problems with the model; the residual velocities become very high, and the X^2/DOF increases by over 10%. The results of Meade and Hager (2005) also suggest that the geodetic data does not support a model with a high slip rate along this portion of the SAF, regardless of the surrounding block geometry. They hypothesize that the discrepancy could be due to a substantial difference in the 10-year rate (*i.e.* our geodetic rate) and the 10,000-year rate (*e.g.* Harden and Matti, 1989); one possible explanation for this difference is that the San Jacinto fault and the Eastern California Shear Zone have accelerated in the late Holocene, thus accommodating a local SAF slip deficit (Meade and Hager, 2005).

In addition to our chosen geologic constraints, we have included several tensile constraints across the model area. To avoid a checkerboard pattern of tensile constraints, *i.e.* alternating high rates of opening and high rates of closing across a series of faults that are understood to be strike slip, the *a priori* tensile slip rate was set to 0.0 ± 1.0 mm/yr on the San Jacinto, Elsinore, Blackwater, Ludlow, Lockhart, Coyote, and Goldstone faults as well as the Parkfield and Mojave segments of the San Andreas fault. These constraints were used in Meade and Hager (2005) as well and are necessary for our model.

3.2 Segment File

The file used to delineate the fault segments in the model is obtained from a combination of the Community Block Model (CBM) and the Community Fault Model (CFM) (Plesch *et al.*, 2004). The CBM is used within the Mojave region, and the CFM incorporates the remainder of the model area. A detailed list of the fault segments in our model can be found in Appendix A.

The faults in the CFM are of extremely high detail, which leads to an increased run time for our model. Because small changes in the fault geometry only affect the elastic deformation in the immediate vicinity of the fault, the detail of the CFM faults is unnecessary. For very small segments in the CFM, lines were merged to create longer fault segments. "Very small" describes a segment in which the change in latitude and the change in longitude total no more than 0.005°. Additionally, when two adjacent fault segments had similar slopes, the segments were merged to create one longer fault segment. Eliminating these segments aids the model by decreasing the run time as well as reducing the number of outliers in the results, thus increasing the fit of the model to the data.

4. Results

Our results are given in Table 2. We provide slip rates for both our geodetic model and our joint geologic and geodetic model. Our joint geologic and geodetic model is our preferred model and gives slip rate estimates consistent with geologic observations throughout southern California, with a few glaring exceptions discussed below.

4.1 Geodetic weighted least squares inversion

After importing the CBM/CFM segments into our model, we performed a purely geodetic weighted least squares inversion of the velocity data using *blocks_sp1*. We maintained *a priori* tensile constraints of 0.0 ± 1.0 mm/yr, as in Meade and Hager (2005), in order to avoid checkerboarding of tensile slip rates. For comparison, the slip rate results from Meade and Hager can be found in Table 3.

One difference in the geodetic models is in the Transverse Ranges. Figure 11 shows the resulting velocity field when the residual velocities of our geodetic model are subtracted from the residual velocities of Meade and Hager (2005). Near the San Cayetano and Santa Susana faults, the two geodetic models produce drastically different residual velocities, evident by the ~5 mm/yr vector pointing to the northeast. The slip rates of the two models differ substantially in this area; our model assigns a thrust rate of 3.5 ± 2.2 mm/yr to the Santa Susana fault, while Meade and Hager estimate a thrust rate of 12.4 ± 2.5 mm/yr.

Fault Name	Geodetic Strike Slip Rate	Joint Geologic/ Geodetic Strike Slip Rate	Geodetic Dip Slip Rate	Joint Geologic/ Geodetic Dip Slip Rate	Geodetic Tensile Slip Rate	Joint Geologic/ Geodetic Tensile Slip Rate
Avawatz	-0.4 ± 4.4	1.7 ± 4.3	20.0 ± 7.2	27.1 ± 7.2	--	--
Big Bend	-22.8 ± 1.9	-18.5 ± 1.8	--	--	-3.0 ± 1.6	1.2 ± 1.4
Blackwater	-0.6 ± 0.7	-1.5 ± 0.6	--	--	0.8 ± 1.5	1.8 ± 1.2
Calico	-11.7 ± 0.9	-12.8 ± 0.8	--	--	2.9 ± 1.7	5.3 ± 1.3
Channel Islands	-2.6 ± 1.5	-2.5 ± 1.5	--	--	-3.1 ± 2.2	-3.2 ± 2.1
Chino	-1.0 ± 0.9	-0.5 ± 0.8	-0.2 ± 1.3	-1.3 ± 0.2	--	--
Coastal Ranges Split	-12.0 ± 1.8	-11.2 ± 1.7	--	--	2.4 ± 1.2	2.2 ± 1.1
Coronado Banks	-3.6 ± 2.7	-3.9 ± 2.7	4.9 ± 4.7	5.9 ± 4.6	--	--
Coyote Lake	-2.0 ± 2.0	-6.7 ± 2.0	--	--	-6.7 ± 2.9	-6.9 ± 2.6
Cucamonga	0.8 ± 1.8	2.6 ± 1.7	3.3 ± 1.5	3.5 ± 1.4	--	--
Death Valley	-2.3 ± 1.9	-1.6 ± 1.8	--	--	-2.8 ± 1.2	-3.9 ± 1.1
Elsinore	-2.1 ± 0.2	-2.1 ± 0.1	--	--	0.1 ± 0.6	0.1 ± 0.5
Furnace Creek	-2.9 ± 1.4	-2.3 ± 1.4	--	--	-0.2 ± 0.9	-0.6 ± 0.9
Garlock West	2.2 ± 1.7	3.1 ± 1.5	--	--	5.7 ± 2.3	6.5 ± 2.2
Garlock Central	4.2 ± 0.2	7.1 ± 0.1	--	--	2.8 ± 2.3	4.2 ± 1.8
Garlock East	8.9 ± 3.6	12.8 ± 3.5	--	--	1.3 ± 3.3	1.7 ± 3.1
Glen Ivy South	-2.1 ± 0.1	-2.1 ± 0.1	--	--	0.2 ± 0.7	0.2 ± 0.5
Glen Ivy North	-0.9 ± 1.2	-0.7 ± 1.1	0.9 ± 1.3	-0.4 ± 0.3	--	--
Goldstone	-10.1 ± 1.0	-11.3 ± 1.0	--	--	-0.9 ± 3.9	-1.0 ± 3.8
Helendale	-2.2 ± 0.9	-0.8 ± 0.8	--	--	0.2 ± 1.2	-2.6 ± 0.0
Hidalgo	-10.9 ± 0.7	-12.2 ± 0.6	--	--	-3.9 ± 1.6	-4.0 ± 1.2
Holser	7.6 ± 1.8	7.9 ± 1.8	--	--	2.9 ± 2.8	2.3 ± 2.8
Hosgri - San Simeon	-4.7 ± 0.5	-5.0 ± 0.5	5.5 ± 1.4	5.4 ± 1.1	--	--
Hunter Mountain	-2.6 ± 1.2	-3.2 ± 1.1	--	--	-0.1 ± 1.0	1.9 ± 0.9
Little Lake	-13.9 ± 2.8	-7.6 ± 2.7	--	--	-2.3 ± 2.9	-0.2 ± 2.7
Lockhart	-2.3 ± 1.1	-1.1 ± 0.7	--	--	-0.6 ± 1.2	-3.0 ± 0.2
Ludlow	-4.7 ± 1.5	-5.5 ± 1.5	--	--	2.3 ± 2.2	2.1 ± 2.2
Newport – Inglewood	-2.1 ± 1.1	-1.9 ± 1.0	--	--	3.9 ± 1.2	2.0 ± 0.3
North Frontal Zone - East	-0.5 ± 1.5	3.4 ± 0.9	16.0 ± 2.3	6.1 ± 1.2	--	--
North Frontal Zone - West	2.2 ± 2.1	4.3 ± 0.6	9.8 ± 2.9	1.6 ± 0.7	--	--
Oak Ridge - Onshore	14.2 ± 1.6	13.8 ± 1.6	9.7 ± 2.6	9.9 ± 2.5	--	--
Oceanside	-2.2 ± 2.3	-2.2 ± 2.3	--	--	0.5 ± 2.2	-0.3 ± 2.1
Owens Valley South	-4.1 ± 1.4	-2.6 ± 1.0	--	--	-1.9 ± 1.1	-6.4 ± 0.9
Palos Verdes	-1.6 ± 1.5	-1.3 ± 1.4	-1.9 ± 3.3	0.0 ± 2.1	--	--
Panamint Valley	-2.5 ± 1.4	-3.4 ± 1.3	-1.1 ± 2.5	0.2 ± 2.3	--	--
Puente Hills	-1.7 ± 0.8	-1.7 ± 0.8	1.4 ± 1.1	2.6 ± 0.9	--	--
Pinto	1.6 ± 2.1	-1.0 ± 1.9	--	--	-1.7 ± 1.9	-4.4 ± 1.8
Raymond	-0.4 ± 1.0	0.1 ± 0.8	5.0 ± 3.2	4.4 ± 3.0	--	--
Red Mountain	-4.0 ± 1.8	-4.6 ± 1.7	2.7 ± 4.3	2.5 ± 4.3	--	--
Rose Canyon	-0.4 ± 1.8	-0.2 ± 1.8	--	--	3.4 ± 1.6	2.0 ± 1.6
San Andreas Fault – North	-37.6 ± 0.6	-37.7 ± 0.5	--	--	1.4 ± 0.4	1.1 ± 0.4
SAF – Parkfield / N.Carrizo	-34.3 ± 0.2	-34.1 ± 0.2	--	--	0.4 ± 0.4	0.5 ± 0.0
SAF – S. Carrizo	-24.4 ± 2.1	-24.3 ± 2.1	--	--	4.4 ± 2.0	5.8 ± 1.9
SAF – Mojave	-19.8 ± 1.3	-18.6 ± 1.2	--	--	-0.3 ± 2.0	0.0 ± 1.9
SAF – San Bernardino	1.8 ± 1.7	-9.5 ± 1.4	--	--	-4.9 ± 2.1	0.8 ± 0.6
SAF – Salton Sea	-17.3 ± 1.6	-22.1 ± 1.6	--	--	-0.2 ± 1.2	0.0 ± 0.9
SAF – Imperial	-38.9 ± 0.8	-38.7 ± 0.8	--	--	-6.7 ± 0.5	-6.6 ± 0.4

Fault Name	Geodetic Strike Slip Rate	Joint Geologic/ Geodetic Strike Slip Rate	Geodetic Dip Slip Rate	Joint Geologic/ Geodetic Dip Slip Rate	Geodetic Tensile Slip Rate	Joint Geologic/ Geodetic Tensile Slip Rate
SAF – Cerro Prieto	-40.9 ± 5.9	-40.9 ± 5.7	--	--	-1.5 ± 3.2	-9.1 ± 3.1
San Cayetano	-7.8 ± 1.7	-7.7 ± 1.7	2.0 ± 4.3	1.5 ± 4.3	--	--
San Clemente	-5.4 ± 1.9	-5.6 ± 1.9	--	--	-3.3 ± 1.3	-3.1 ± 1.3
San Gabriel East	1.1 ± 2.0	0.1 ± 1.9	--	--	0.6 ± 1.7	3.1 ± 1.3
San Gabriel West	-0.6 ± 1.9	-0.1 ± 1.9	3.9 ± 2.9	2.6 ± 2.8	--	--
San Jacinto	-18.8 ± 1.0	-15.0 ± 1.0	--	--	-0.9 ± 0.8	-0.8 ± 0.6
Santa Monica Mountains	0.6 ± 1.7	0.6 ± 1.6	-3.1 ± 2.2	-3.4 ± 2.1	--	--
Santa Rosa Island	-3.0 ± 1.3	-2.9 ± 1.3	--	--	2.5 ± 2.4	2.9 ± 2.3
Santa Susana	1.2 ± 1.6	0.9 ± 1.6	3.5 ± 2.2	3.7 ± 2.2	--	--
Sierra Madre	-0.6 ± 1.8	1.9 ± 1.5	4.1 ± 2.8	1.2 ± 1.8	--	--
Sierra Nevada South	2.3 ± 3.5	2.3 ± 3.3	--	--	6.1 ± 3.9	3.1 ± 3.9
Sierra Nevada North	-3.5 ± 0.7	-1.3 ± 0.3	--	--	-1.3 ± 0.5	-1.7 ± 0.5
White Wolf	0.4 ± 1.6	0.3 ± 1.5	2.1 ± 2.9	1.8 ± 2.9	--	--

Table 2: Results for geodetic model (blue) and for model including *a priori* constraints as well as geodetic data (black). All slip rates are in mm/yr units. *A priori* slip rates include Newport-Inglewood (-1.8 ± 0.5 mm/yr), San Andreas – Carrizo (-33.9 ± 2.9 mm/yr), Garlock Central (6.5 ± 2.5 mm/yr), Helendale (-0.8 ± 0.5 mm/yr), Owens Valley (-2.0 ± 1.0 mm/yr), Chino (-0.4 ± 0.1 mm/yr), and Sierra Madre (0.8 ± 0.4 mm/yr, dip slip). Positive values are left-lateral strike slip and convergence. Negative values are right-lateral strike slip and divergence.

Fault name	Strike-slip rate (M & H)	Our strike-slip rate (geodetic)	Dip-slip rate (M& H)	Our dip-slip rate (geodetic)	Tensile-slip rate (M&H)	Our tensile-slip rate (geodetic)
SAF (Parkfield)	-35.5 ± 0.5	-34.3 ± 0.2	--	--	0.1 ± 0.4	0.4 ± 0.4
SAF (Carrizo)	-35.4 ± 0.7	-24.4 ± 2.1	--	--	2.5 ± 0.4	4.4 ± 2.0
SAF (Mojave)	-17.5 ± 1.4	-19.8 ± 1.3	--	--	-1.5 ± 2.1	-0.3 ± 2.0
SAF (San Bernadino)	-4.3 ± 1.5	1.8 ± 1.7	--	--	0.4 ± 1.7	-4.9 ± 2.1
SAF (Salton Sea)	-22.8 ± 0.5	-17.3 ± 1.6	--	--	1.5 ± 0.6	-0.2 ± 1.2
SAF (Imperial)	-36.5 ± 0.6	-38.9 ± 0.8	--	--	-8.5 ± 0.5	-6.7 ± 0.5
SAF (Cerro Prieto)	-40.3 ± 1.5	-40.9 ± 5.9	--	--	-4.3 ± 0.4	-1.5 ± 3.2
Eureka Peak	-21.4 ± 1.6	--	--	--	-4.3 ± 1.0	--
Pinto Mountain	8.5 ± 0.9	1.6 ± 2.1	--	--	-9.3 ± 1.0	-1.7 ± 1.9
San Jacinto	-12.5 ± 1.2	-18.8 ± 1.0	--	--	0.0 ± 0.7	-0.9 ± 0.8
Elsinore	-3.0 ± 0.6	-2.1 ± 0.2	--	--	-0.9 ± 0.7	0.1 ± 0.6
Rose Canyon	-0.5 ± 2.5	-0.4 ± 1.8	--	--	1.1 ± 2.0	3.4 ± 1.6
Oceanside	-1.8 ± 3.2	-2.2 ± 2.3	--	--	2.8 ± 2.8	0.5 ± 2.2
Coronado Bank	-4.8 ± 3.0	-3.6 ± 2.7	--	4.9 ± 4.7	0.1 ± 1.9	--
San Clemente	-3.6 ± 1.6	-5.4 ± 1.9	--	--	-2.9 ± 0.9	-3.3 ± 1.3
Hosgri	-4.0 ± 0.6	-4.7 ± 0.5	--	5.5 ± 1.4	0.7 ± 0.6	--
Agua Blanca	-8.5 ± 2.7	--	--	--	1.1 ± 1.6	--
Newport – Inglewood	-1.0 ± 1.7	-2.1 ± 1.1	--	--	0.5 ± 1.3	3.9 ± 1.2
Palos Verdes	-3.4 ± 1.4	-1.6 ± 1.5	--	-1.9 ± 3.3	3.6 ± 1.5	--
Raymond Hill	2.9 ± 1.0	-0.4 ± 1.0	--	5.0 ± 3.2	0.2 ± 1.7	--
Chino	0.3 ± 1.3	-1.0 ± 0.9	--	-0.2 ± 1.3	-2.8 ± 0.8	--
Puente Hills Thrust	-2.5 ± 1.0	-1.7 ± 0.8	3.2 ± 0.9	1.4 ± 1.1	--	--
Cucamonga	5.1 ± 1.5	0.8 ± 1.8	7.6 ± 1.6	3.3 ± 1.5	--	--
Hollywood Hills	2.9 ± 0.9	--	0.4 ± 1.9	--	--	--
Santa Monica Mtns	2.6 ± 1.4	0.6 ± 1.7	-0.4 ± 2.2	-3.1 ± 2.2	--	--
Sierra Madre (north)	-1.8 ± 1.5	--	9.5 ± 2.4	--	--	--
Sierra Madre (south)	-1.9 ± 1.2	-0.6 ± 1.8	2.7 ± 2.4	4.1 ± 2.8	--	--
Santa Susana	-1.7 ± 1.3	1.2 ± 1.6	12.4 ± 2.5	3.5 ± 2.2	--	--
San Cayetano	-1.8 ± 1.3	-7.8 ± 1.7	4.9 ± 2.1	2.0 ± 4.3	--	--
Oak Ridge	7.3 ± 1.4	14.2 ± 1.6	7.6 ± 2.2	9.7 ± 2.6	--	--
White Wolf	-1.2 ± 1.3	0.4 ± 1.6	3.7 ± 1.7	2.1 ± 2.9	--	--
North Frontal	0.9 ± 1.7	2.2 ± 2.1	5.2 ± 3.0	9.8 ± 2.9	--	--
Coastal Ranges Split	-6.0 ± 1.5	-12.0 ± 1.8	--	--	-1.0 ± 1.0	2.4 ± 1.2
San Gabriel	-1.0 ± 2.3	1.1 ± 2.0	---	--	0.5 ± 2.1	0.6 ± 1.7
Garlock (west)	4.4 ± 1.2	2.2 ± 1.7	--	--	4.4 ± 1.5	5.7 ± 2.3
Garlock (central)	1.1 ± 1.6	4.2 ± 0.2	--	--	0.1 ± 1.4	2.8 ± 2.3
Garlock (east)	0.6 ± 1.9	8.9 ± 3.6	--	--	-5.5 ± 1.4	1.3 ± 3.3
Blackwater-Landers	-2.3 ± 0.7	--	--	--	0.1 ± 1.2	--
Helendale	-1.7 ± 1.0	-2.2 ± 0.9	--	--	-2.3 ± 1.1	0.2 ± 1.2
Goldstone	-13.5 ± 0.8	-10.1 ± 1.0	--	--	0.0 ± 1.4	-0.9 ± 3.9
Eastern Mojave (2)	0.5 ± 0.9	--	--	--	-1.5 ± 0.8	--
Nevada Split	0.7 ± 0.6	--	--	--	-2.5 ± 0.6	--
Airport Lake	-6.7 ± 1.1	--	--	--	1.0 ± 1.5	--
Owens Valley	-3.6 ± 0.9	-4.1 ± 1.4	--	--	-0.5 ± 0.8	-1.9 ± 1.1
Panamint Valley	-3.1 ± 1.3	-2.5 ± 1.4	--	-1.1 ± 2.5	-3.5 ± 1.2	--
Death Valley	-2.6 ± 1.2	-2.3 ± 1.9	--	--	-0.6 ± 0.9	-2.8 ± 1.2
Fish Lake	-6.0 ± 2.1	--	--	--	-1.1 ± 1.0	--

Table 3: Selected slip rates (mm/yr) from Meade and Hager (2005) and our geodetic model. Meade and Hager's rates are from a geodetic model with Mojave block geometries shown in red in Figure 17. Positive values are left-lateral strike slip and convergence. Negative values are right-lateral strike slip and divergence.

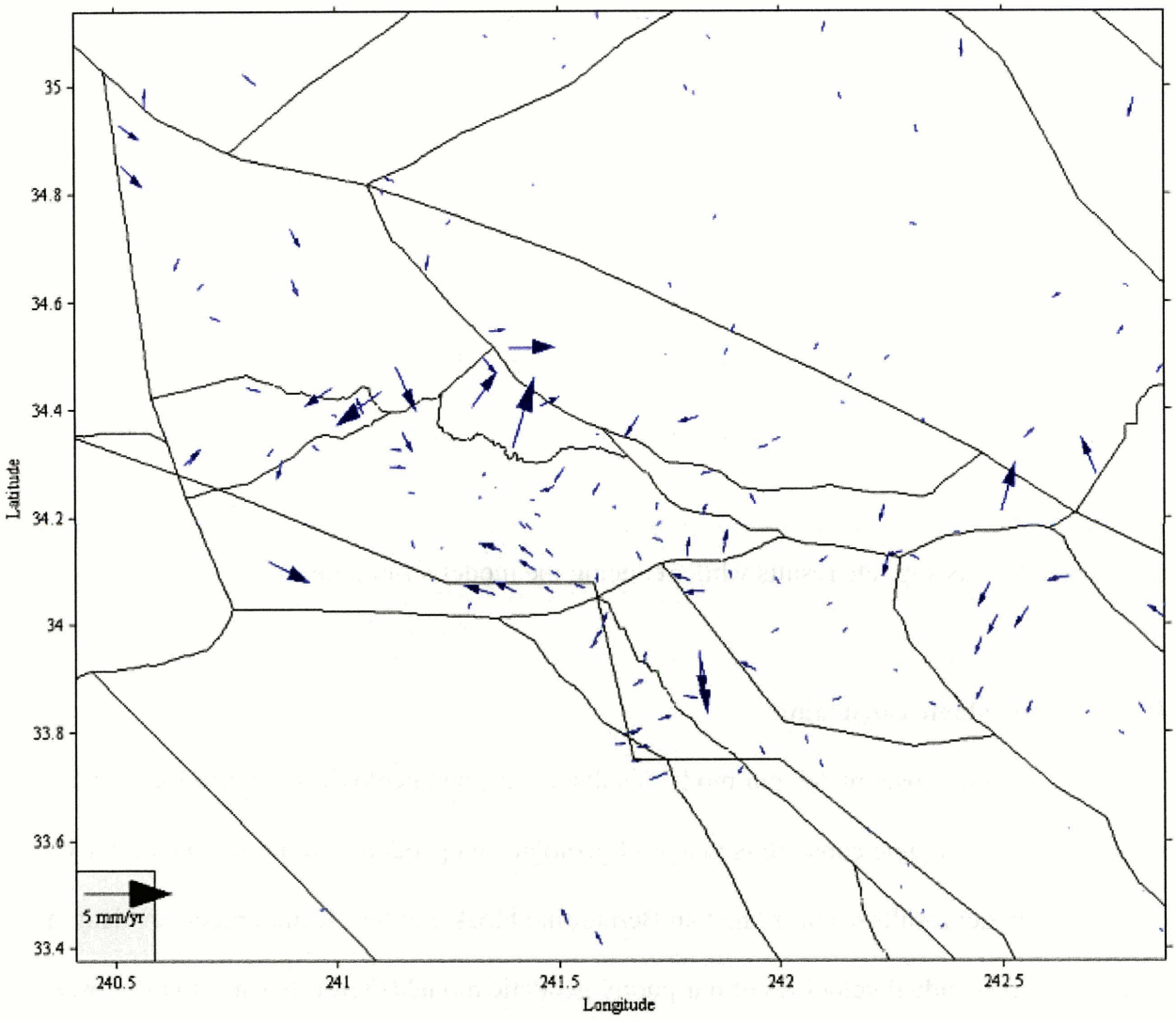

Figure 11: Velocity field showing the difference between the residual velocities in Meade and Hager (2005) and the residual velocities in our geodetic model. The large arrows at 34.4 N represent substantial differences in the residual data near the Santa Susana and San Cayetano faults. In the San Jacinto block, it is evident that the block has a slight difference in rotation rate between the two models.

Also evident in Figure 11 is a difference in rotation of the northern San Jacinto block located at approximately (34N, 242.5E). The counterclockwise trend of these velocity vectors suggest that our San Jacinto slip rate may be faster than Meade and Hager's. As expected, results along the San Jacinto fault differ between the two models; our geodetic model estimates a right lateral slip of 18.8 ± 1.0 mm/yr, and Meade and Hager estimate 12.5 ± 1.2 mm/yr.

Because our model differs from Meade and Hager solely in block geometry, a comparison of the two models will show how *blocks_sp1* can be used to contrast slip rate estimates from different geometric configurations. We subtract the residual velocities of our model from the residual velocities of Meade and Hager to show where the two models disagree (Figure 12).

In areas where the geometries of the two models are similar (*e.g.* Death Valley), the differences in both the residual and model velocities are minimal; thus, a more realistic fault trace will produce results similar to a simplified geometry. In other words, an overly complicated fault geometry will only have a major effect on the run time of the model. A simpler model can provide analogous slip rate results while reducing the model's run time.

4.2 Adding geologic constraints

In order to closer match our model results to expected geologic slip rates, we included several *a priori* geologic constraints in a joint geologic and geodetic inversion. The primary changes in model results occur in the San Bernardino block and San Jacinto block, evident in Figure 13. The residual velocities of our purely geodetic model (Figure 14) are slightly lower than the residual velocities of our joint geologic and geodetic model (Figure 15), evident in the slight increase (6%) in X^2/DOF, from 2.062 to 2.189. However, given that the changes in residual velocities are minimal, we conclude that imposing our *a priori* constraints on our geodetic model does not jeopardize the statistical significance of our results.

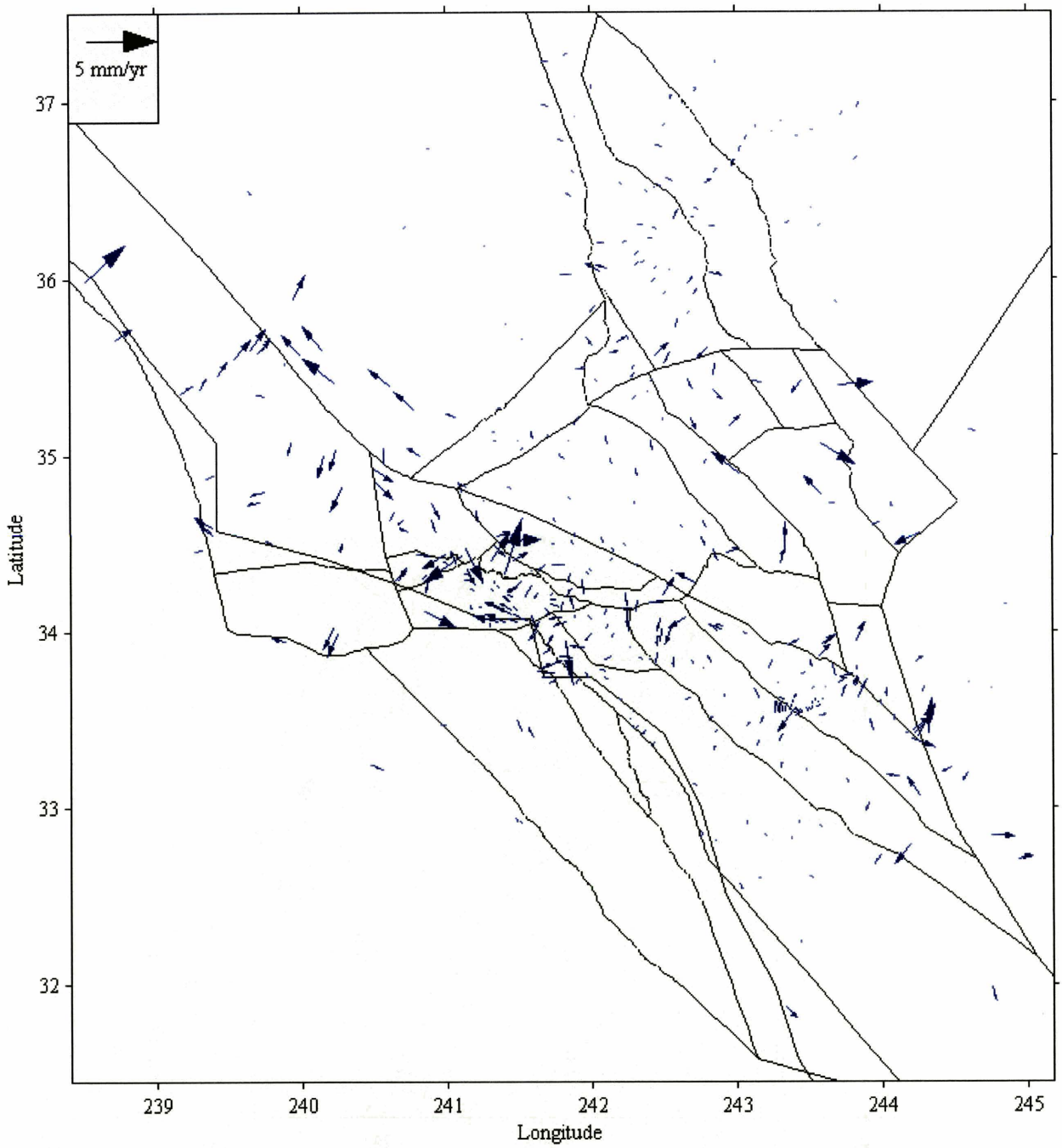

Figure 12: Arrows show the difference between the residual velocities of Meade and Hager (2005) and the residual velocities of our geodetic model. The residual velocities of the models are similar in the majority of the Eastern California Shear Zone, with major differences occurring in the Transverse Ranges and near the Parkfield area of the SAF.

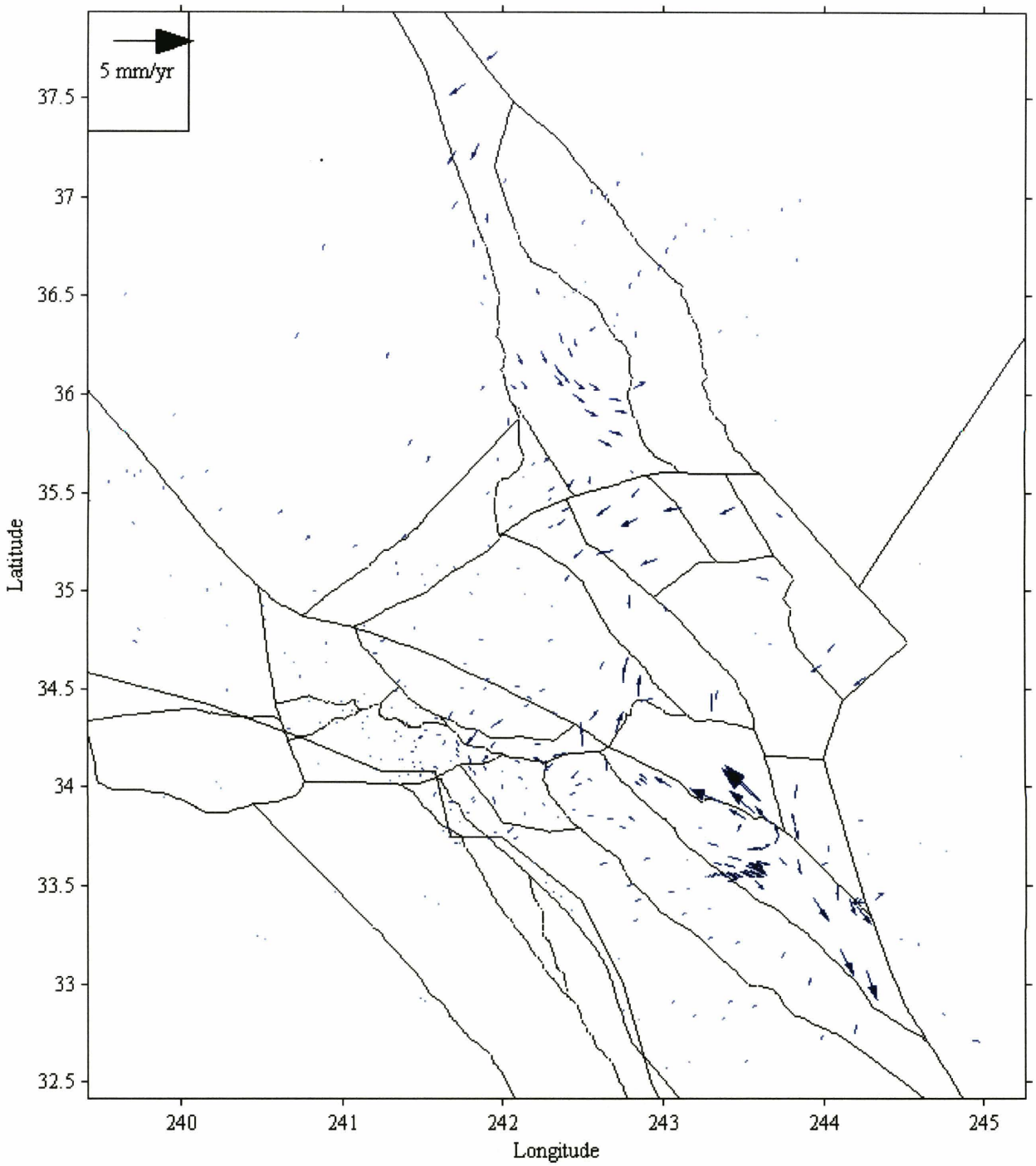

Figure 13: Resulting velocity vectors when residual velocities of our geodetic model are subtracted from residual velocities of our joint geologic and geodetic model. It is clear that the primary discrepancies between the two sets of residual velocities occur in the San Jacinto and San Bernardino blocks. Our *a priori* geologic rates along the SAF – San Bernardino and the North Frontal fault zone result in significant differences between the models near the SAF – San Bernardino area; these differences propagate into the San Jacinto block. Similarly, the Owens Valley block has an obvious difference in rotation rate between the two models.

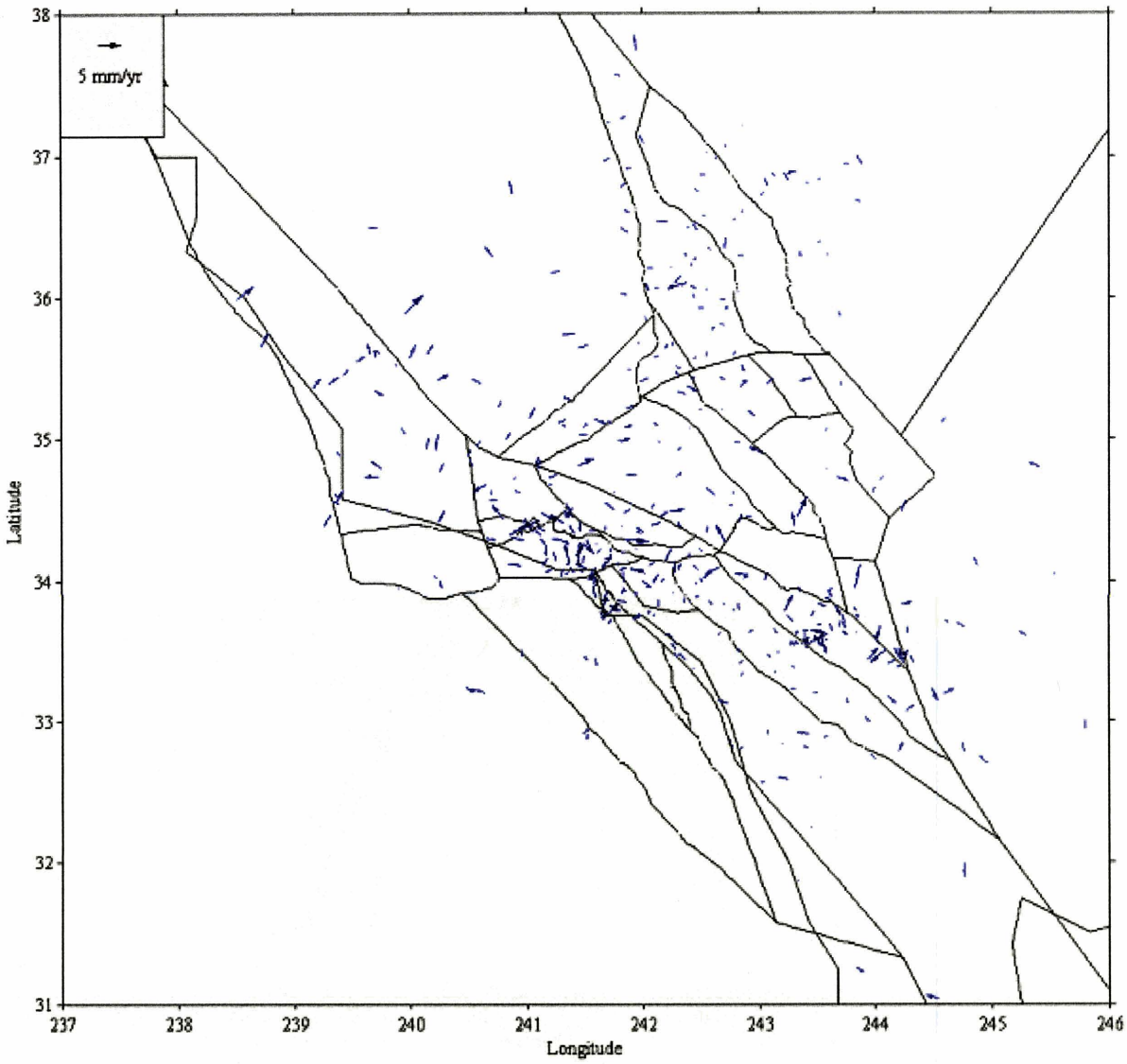

Figure 14: Residual velocities for our geodetic model. The smaller blocks in the Transverse Ranges have a high density of velocity stations and display residual velocities up to 5 mm/yr.

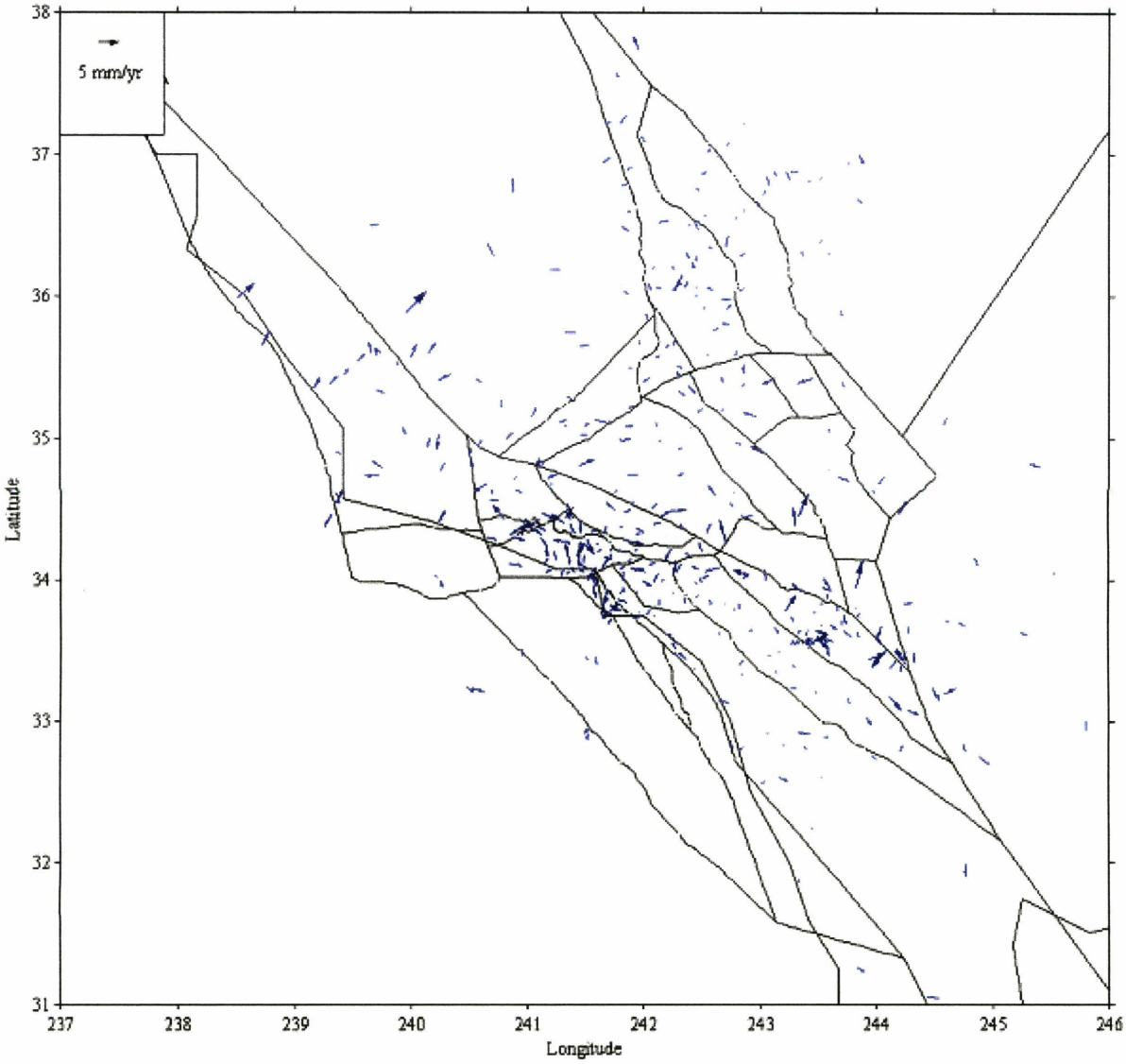

Figure 15: Residual velocities of our joint geologic and geodetic model. Velocity vectors are typically under 5 mm/yr, although there are several instances where the residual rates are slightly higher.

4.2.1 San Andreas Fault

Between our geodetic model and our joint geologic and geodetic model, the slip rates along the SAF do not vary substantially to the north of the San Bernardino Mountains or to the south of the Salton Sea block. Both models have *a priori* tensile constraints of 0.0 ± 1.0 mm/yr along the SAF in the Mojave and near Parkfield. Our joint geologic and geodetic model has an

additional *a priori* constraint of 33.9 ± 2.9 mm/yr (right lateral slip) along the SAF near the Parkfield / N. Carrizo area.

Variation along the SAF between our two models occurs along the SAF – San Bernardino Mountains as well as the SAF – Salton Sea. The changes in both segments are due to *a priori* constraints imposed upon the San Bernardino block, which will be discussed below.

Our joint model estimates a slip rate of 37.7 ± 0.5 mm/yr along our northernmost SAF, 34.1 ± 0.2 mm/yr near Parkfield and the N. Carrizo area, 24.3 ± 2.1 mm/yr along the S. Carrizo area, 18.6 ± 1.2 mm/yr for the SAF – Mojave, 9.5 ± 1.4 mm/yr for the SAF – San Bernardino, 22.1 ± 1.6 mm/yr near the Salton Sea, 38.7 ± 0.8 mm/yr for the SAF – Imperial, and 40.9 ± 5.7 mm/yr along the SAF – Cerro Prieto. Our Parkfield and Carrizo rates agree with Sieh and Jahns (1984). Sieh (1984) found a minimum slip rate of 9 mm/yr in the Mojave area, but other studies within the Mojave area estimate SAF slip rates of 30-40 mm/yr (*e.g.* Salyards *et al.*, 1992).

4.2.2 San Bernardino Mountains

The SAF is somewhat complex in the San Gorgonio Pass area near the San Bernardino Mountains, splaying into a north and a south branch just east of the city of San Bernardino (Petersen and Wesnousky, 1994), but the SAF is understood to still have at least 11 mm/yr right lateral slip in this region (Harden and Matti, 1989). Our geodetic model displays a left lateral slip rate of 1.8 mm/yr along the SAF in this area (Figure 10). However, in our joint geologic and geodetic model, we have assigned a loose geologic constraint of 10.0 ± 10.0 mm/yr right lateral slip to the SAF to force the resulting model slip rates to better conform to field observations. Furthermore, because constraining the SAF has an effect on the surrounding faults, we also assigned a loose geologic constraint of 3.0 ± 3.0 mm/yr thrust on the North Frontal Zone to force

it to maintain a low thrusting rate (Jennings, 1994). Including these constraints in our joint geologic and geodetic inversion model results in a right lateral slip rate of 9.5 ± 1.4 mm/yr along this segment of the SAF. This rate is significantly higher than the rate given by Meade and Hager, but it still falls short of the rates measured by Harden and Matti. However, given the limited number of velocity stations within the San Bernardino block as well as the fact that the area is somewhat geologically complex and uncertain, we accept the low slip rates resulting from the joint geologic and geodetic model.

4.2.3 Garlock and White Wolf Faults

Based on seismicity depths given in Petersen and Wesnousky (1994), we have assigned a locking depth of 25 km to the westernmost segment of the Garlock fault, with the locking depths for the remaining segments set to 15 km. Our geodetic model shows an average left lateral slip rate of 4.2 ± 2.3 mm/yr along the Garlock fault (with the rate increasing as the fault progresses from west to east), as well as a thrust rate of 2.1 ± 2.9 mm/yr along the White Wolf fault. Our joint geologic and geodetic model, which includes a geologic constraint of 6.5 ± 2.5 mm/yr (left lateral slip), gives an overall average result of 6.5 ± 2.0 mm/yr along the Garlock fault and 1.8 ± 2.9 mm/yr along the White Wolf fault. In both models, the strike-slip rate along the White Wolf fault is minimal.

The Garlock fault can be further subdivided into West, Central, and East segments. The westernmost portion, which separates the White Wolf and Mojave blocks, has a relatively low slip rate of 2.2 ± 1.7 mm/yr in our geodetic model and 3.1 ± 1.5 mm/yr in our joint geologic and geodetic model. The central Garlock contains an *a priori* geologic constraint of 6.5 ± 2.5 mm/yr in our joint geologic and geodetic model, increasing its geodetic model slip rate of 4.2 ± 0.2

mm/yr to a joint model slip rate of 7.1 ± 0.1 mm/yr. A higher slip rate occurs along the eastern Garlock, with an average slip of 8.9 ± 3.6 mm/yr in our geodetic model and 12.8 ± 3.5 mm/yr in our joint geologic and geodetic model.

4.2.4 Palos Verdes and Coronado Banks Faults

Our results along the Palos Verdes fault zone and Coronado Banks fault zone are consistent with Jennings (1994). These faults dip to the northeast and are subdivided by the Oceanside fault (Figure 16). The sense of motion along these faults is not known well, but

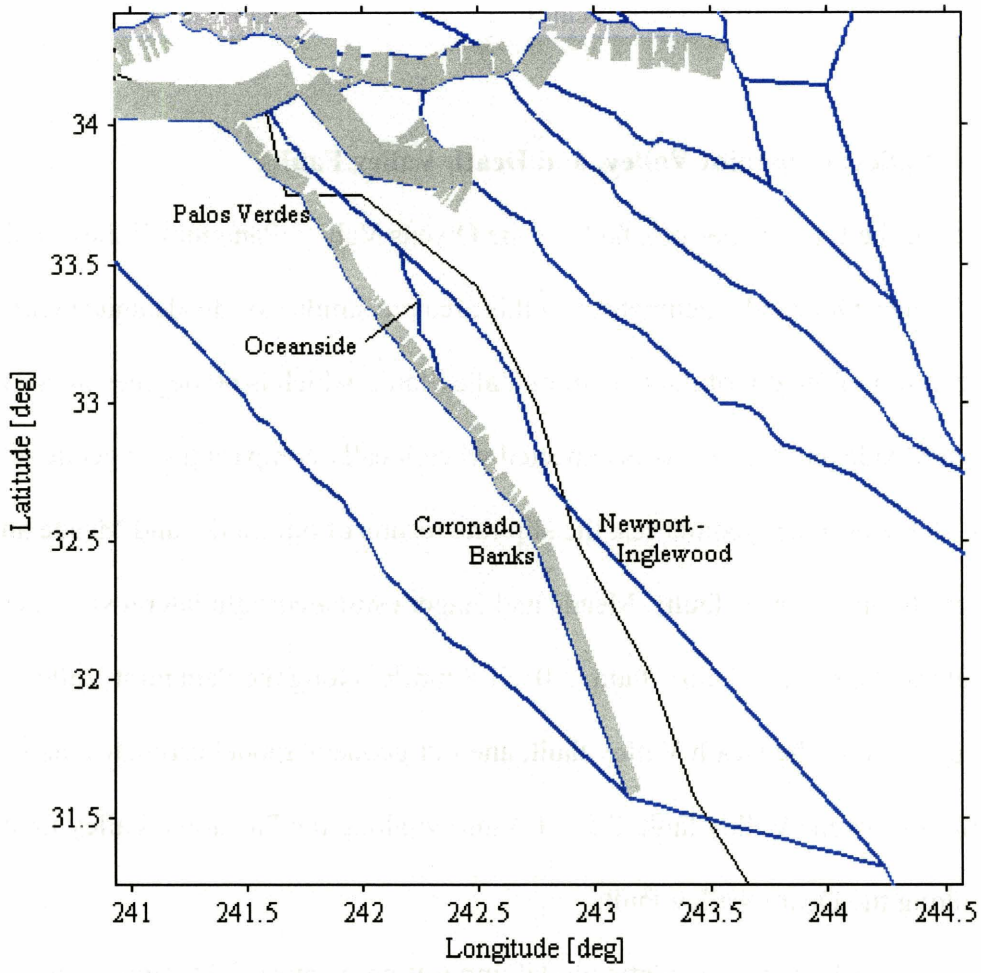

Figure 16: The Palos Verdes and Coronado Banks fault zones dip to the northeast are split by the Oceanside fault. Our model results show an thrusting along the Coronado Banks fault zone and an uncertain sense of dip slip along the Palos Verdes fault zone.

Jennings (1994) estimated right lateral slip along both faults, with a questionably thrusting sense of motion along the Palos Verdes fault zone and a questionably normal sense of motion along the Coronado Banks fault zone. Our geodetic model has right lateral slip along both faults, with an additional thrust component on the Coronado Banks fault zone. The Palos Verdes fault zone has a normal component of 1.9 ± 3.3 mm/yr, but given the uncertainty on this value, our geodetic model cannot give conclusive evidence toward either a normal or thrusting sense of dip slip motion. Our joint geologic and geodetic model gives similar results, with both faults having right lateral slip as well as a thrusting sense of dip slip motion along the Coronado Banks fault zone and an uncertain sense of dip slip motion along the Palos Verdes fault zone.

4.2.5 Owens Valley, Panamint Valley, and Death Valley Faults

North of the Eastern Garlock fault lie the Owens Valley, Panamint Valley, and Death Valley fault zones. Our model geometries in this area are similar to Meade and Hager (2005), with the exception of the dip of the Panamint Valley fault, which is 60 degrees in our model and 90 degrees in Meade and Hager. As is expected when locally comparing two geodetic models with nearly identical block geometries, the slip rate results of our model and Meade and Hager's model are similar along these faults. Meade and Hager estimated right lateral slip rates of 3.8 ± 0.8 mm/yr along the Owens Valley fault, 3.0 ± 1.3 mm/yr along the Panamint Valley fault, and 2.3 ± 1.2 mm/yr along the Death Valley fault, and our geodetic model estimates rates of 4.1 ± 1.4 mm/yr along the Owens Valley fault, 2.5 ± 1.4 mm/yr along the Panamint Valley fault, and 2.3 ± 1.9 mm/yr along the Death Valley fault.

Our joint geologic and geodetic model imposes an *a priori* right lateral slip rate constraint of 2.0 ± 1.0 mm/yr on one segment of the Owens Valley fault, resulting in overall right lateral

slip rates of 2.6 ± 1.0 mm/yr along the Owens Valley fault, 1.6 ± 1.8 mm/yr along the Death Valley fault, and 3.4 ± 1.3 mm/yr along the Panamint Valley fault. The constraint on the Owens Valley fault changes the rotation rate of the Owens Valley block, evident in Figure 13. For the Owens Valley and Death Valley faults, our joint geologic and geodetic model results are closer to expected geologic rates than the purely geodetic model results. The magnitudes of the residual vectors are similar (Figures 14 and 15), but their directions are different (Figure 13), showing that the two models provide a similar fit to the local geodetic data.

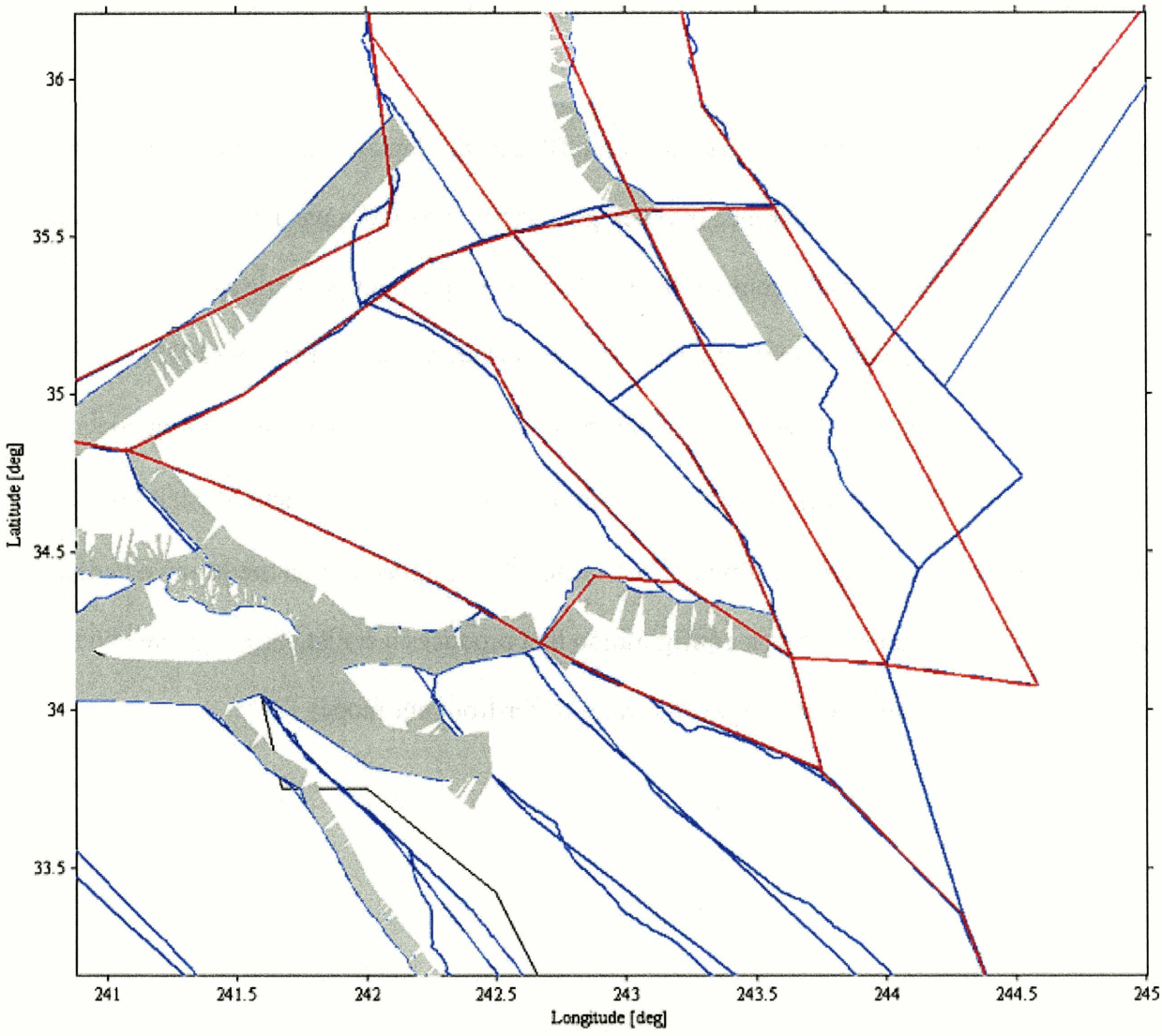

Figure 17: Fault segments within the Mojave area. Segments in red delineate the geometry of Meade and Hager (2005). Segments in blue are our fault selections.

4.2.6 Mojave area

Figure 17 shows the Mojave block geometry from Meade and Hager (2005) superimposed onto our geometry. The locations of the San Andreas and Garlock faults are nearly identical (with the exception of the SAF in the San Bernardino Mountains area). The Lockhart, Helendale, North Frontal, and Death Valley faults are also quite similar between the two models.

The most striking difference between the models is in the eastern Mojave. In addition to the inclusion of the Coyote Lake and Ludlow faults in our model, the locations of the Blackwater and Avawatz faults vary greatly between the models. Furthermore, we have selected the Calico fault rather than the Landers fault to connect the Blackwater fault to the North Frontal fault zone.

Despite the drastic difference in block geometries in the Mojave area, both models in Figure 17 produce statistically comparable results. We adapted our geodetic model by replacing our Mojave area segments with the Mojave segments from Meade and Hager (2005). The resulting X^2/DOF was 2.181, which is higher than the resulting X^2/DOF from our geodetic model, but still lower than the X^2/DOF from our joint geologic and geodetic model. From the residual velocities and resulting slip rates in Figure 18, it is apparent that the Mojave geometry of Meade and Hager is another block configuration that produces a statistically feasible geodetic model, although its fault locations and slip rates differ from our model.

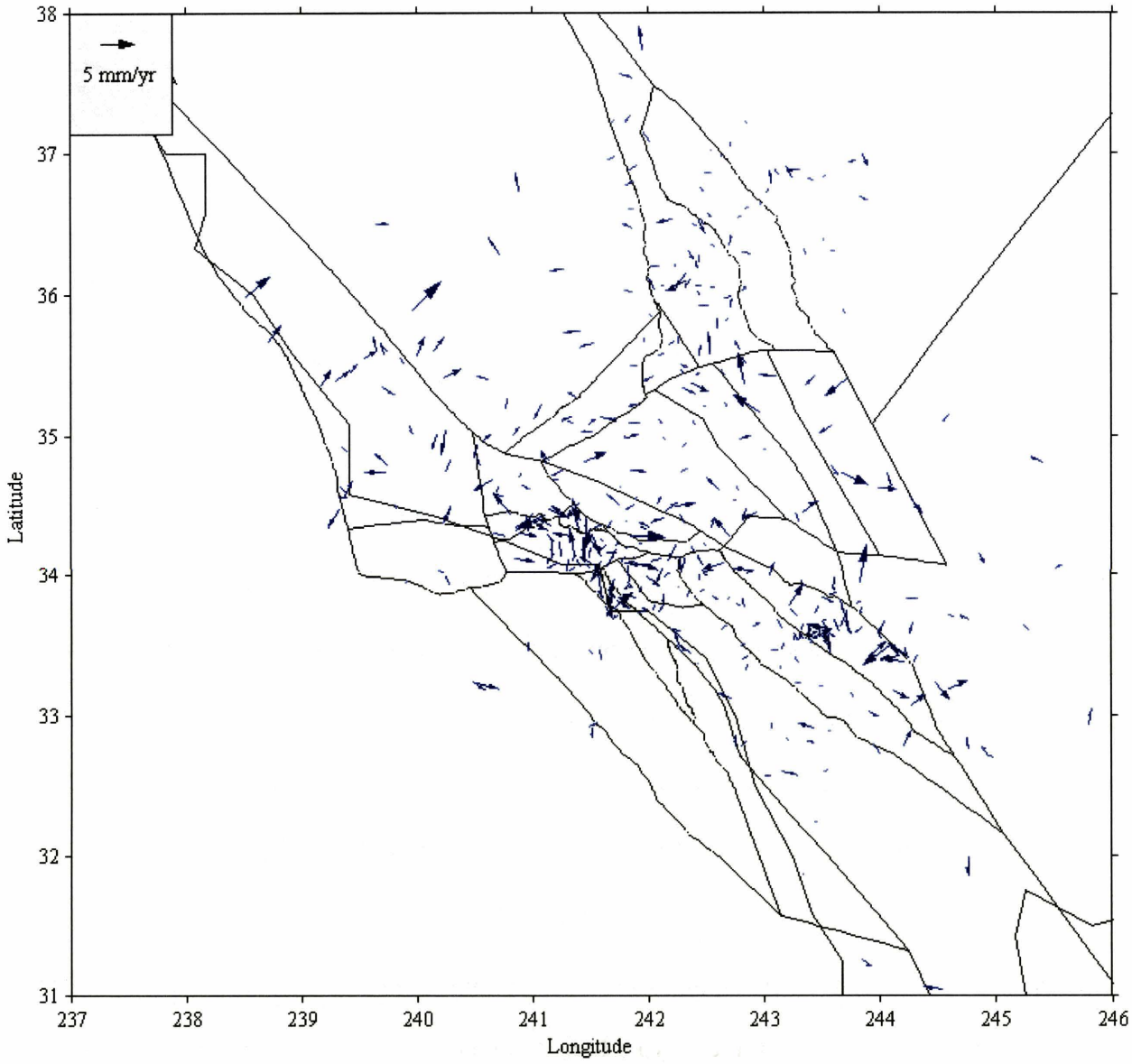

Figure 18: Residual velocities of our model with Meade and Hager's geometry within the Mojave area. The residual velocity vectors are small enough to consider this a statistically acceptable block geometry.

In areas of the Mojave where velocity data is sparse, our *a priori* geologic constraints help refine our geodetic slip rate model results. We have included a left lateral slip constraint of 6.5 ± 2.5 mm/yr along the Garlock fault and a right lateral slip constraint of 0.8 ± 0.5 mm/yr along the Helendale fault, as well as our previously stated constraints on the San Bernardino block. We expect that the changes in our results are due to the inclusion of these near-field

Fault Name	Geodetic Strike Slip Rate	Joint Geologic/ Geodetic Strike Slip Rate	Relative Change	Geodetic Tensile Slip Rate	Joint Geologic/ Geodetic Tensile Slip Rate	Relative Change
Blackwater	-0.6 ± 0.7	-1.5 ± 0.6	Right Lateral	0.8 ± 1.5	1.8 ± 1.2	Closing
Calico	-11.7 ± 0.9	-12.8 ± 0.8	Right Lateral	2.9 ± 1.7	5.3 ± 1.3	Closing
Goldstone	-10.1 ± 1.0	-11.3 ± 1.0	Right Lateral	-0.9 ± 3.9	-1.0 ± 3.8	Opening
Helendale	-2.2 ± 0.9	-0.8 ± 0.8	Left Lateral	0.2 ± 1.2	-2.6 ± 0.0	Opening
Hidalgo	-10.9 ± 0.7	-12.2 ± 0.6	Right Lateral	-3.9 ± 1.6	-4.0 ± 1.2	Opening
Lockhart	-2.3 ± 1.1	-1.1 ± 0.7	Left Lateral	-0.6 ± 1.2	-3.0 ± 0.2	Opening
Ludlow	-4.7 ± 1.5	-5.5 ± 1.5	Right Lateral	2.3 ± 2.2	2.1 ± 2.2	Opening

Table 4: Slip rates of selected faults in the Mojave Area. "Relative Change" refers to the change in the model results when *a priori* geologic constraints are imposed. A right lateral change means the slip rate has shifted to either a higher right lateral (negative) rate or a lower left lateral (positive) rate. Similarly, a left lateral change occurs when the slip rate has shifted to either a higher left lateral rate or a lower right lateral rate. "Closing" means the tensile rate becomes more positive with *a priori* constraints, and "Opening" refers to a more negative tensile rate.

constraints (rather than other far-field constraints). Table 4 highlights the changes in selected Mojave area faults.

It is evident that the strike slip rates along the Hidalgo, Calico, and Goldstone faults are quite high when compared with the Blackwater, Lockhart, Helendale, and Ludlow faults. The strike slip rate along the Goldstone fault in Meade and Hager (2005) is similarly high (-13.5 ± 0.8 mm/yr). We agree with Meade and Hager that these high rates suggest that the majority of the relative motion between the North American and Pacific plates that is accommodated within the Mojave area is concentrated to the east of the Blackwater fault. However, because our block geometries differ to the south of the Coyote Lake fault, our slip rates along the Calico and Hidalgo faults are much higher than Meade and Hager's rate along their Blackwater and Landers faults. The motion that is accommodated solely by the Goldstone fault in Meade and Hager's model is transferred westward to the Calico and Hidalgo faults in our model.

The Calico and Hidalgo faults are expected to produce similar strike slip results because they are connected in a continuous set of segments in our model. Not enough velocity stations exist within the Calico block to determine its rotation direction, but the tensile slip rates on the

Calico and Hidalgo faults suggest that the block is rotating counterclockwise, *i.e.* converging in the north and diverging in the south along the Calico-Hidalgo boundary.

5. Conclusions and Future Work

The CBM and CFM can still be adapted to accommodate the nuances of our modeling scheme. In particular, our model is better suited to slightly larger blocks than given in the CBM, particularly in areas with sparse geodetic data. Along the same lines, a simpler fault geometry that maintains the general block shape and relative velocity station locations will produce quality results in a more efficient manner. The next step to refine our model and make it more user-friendly is to import the entire CBM to reduce the number of fault segments. If the smaller blocks of the CBM still appear necessary to produce realistic results, we can impose more geologic constraints in the absence of sufficient geodetic data.

Our model suggests that the faults in the Mojave area account for a significant portion of the relative motion between the Pacific and North America plates. The eastern Mojave area (within the Calico block) appears to be accommodating a large part of this motion through strike slip faulting along the Calico and Hidalgo faults as well as the Goldstone fault. Because these faults are not well-constrained geologically and the velocity data in the area are sparse, it is possible that there are other faults in the Mojave that account for some of this motion, and we have simply not included them in our model. However, our data and block configurations predict a high overall slip rate east of the Blackwater fault.

The San Andreas fault is moving slowly in the San Bernardino Mountains area; the lost right-lateral slip rate is accommodated in our model by a higher slip rate along the San Jacinto fault as well as in the eastern Mojave area. Our slip rate of 9.5 ± 1.4 mm/yr is lower than rates

that have been previously observed in the field. This area lacks a satisfactory array of velocity stations, and it would be prudent to obtain a more complete data set to find out if indeed this part of the SAF is moving so slowly on a geodetic time scale. This area deserves more attention in order to determine whether or not a significant local seismic hazard exists.

In addition to the low slip rate along the SAF, we find evidence of two structures in the Coastal Ranges that are unaccounted for in the CBM. These structures represent deformation that is not expressed as a surface rupture. We find that dividing the CBM's Coastal Range block into three blocks provides a more statistically accurate set of model results.

Once a block model is obtained that sufficiently satisfies the geodetic data, *a priori* geologic constraints can refine the model in areas where geodetic data is sparse. However, more widespread coverage of reliable velocity stations will give more consistent results and provide evidence for more recent seismic hazard risks that aren't apparent in long term geologic rates. The model should maintain general consistency with well known long term geologic rates, but only if the residual velocities and X^2/DOF remain low enough so that the model is still statistically significant. Our results are a step along the path toward a reliable seismic hazard model.

6. References

Atwater, Tanya (1970). Implications of plate tectonics for the Cenozoic tectonic evolution of Western North America, *Geological Society of America Bulletin* **81**, 3513-3536.

Bird, Peter and Robert W. Rosenstock (1984). Kinematics of present crust and mantle flow in southern California, *Geological Society of America Bulletin* **95**, 946-957.

Bird, Peter, and Xianghong Kong, Computer simulations of California tectonics confirm very slow strength of major faults, *Geol. Soc. Am. Bull.*, *106*, 159 - 174, 1994.

Cheng, Abe, David D. Jackson, and Mitsuhiro Matsu'ura (1987). Aseismic crustal deformation in the Transverse Ranges of southern California, *Tectonophysics* **144**, 159-180.

Dokka, R. K. and C. J. Travis (1990a). Lake Cenezoic strike-slip faulting in the Mojave Desert, California, *Tectonics* **9**, 311-340.

Dokka, R. K. and C. J. Travis (1990b). The role of the eastern California shear zone, *Geophysical Research Letters* **17**, 1323-1327.

Fischer, P. J. and G. I. Mills (1991). The offshore Newport-Inglewood-Rose Canyon fault zone, California: Structure, segmentation and tectonics in *Environmental Perils San Diego Region*, P.L. Abbott and W.J. Elliott (Editors), San Diego Association of Geologists, San Diego, 17-36.

Harden, J.W. and J.C. Matti (1989). Holocene and late Pleistocene slip rates on the San Andreas Fault in Yucaipa, California, using displaced alluvial-fan deposits and soil chronology, *Geological Society of America Bulletin* **101**, 1107-1117.

Hauksson, E., 2000, Crustal structure and seismicity distribution adjacent to the Pacific and North American plate boundary in southern California, Journal of Geophysical Research, **105**, no. B6, 13,875-13,903.

Jennings, Charles W. (1994). Fault Activity Map of California and Adjacent Areas with Location and Ages of Recent Volcanic Eruptions. *California Geologic Data Map Series, Map No. 6*, California Division of Mines and Geology.

Meade, Brendan J. and Bradford H. Hager (2005). Block models of crustal motion in southern California constrained by GPS measurements, *Journal of Geophysical Research* **110**, B03403, doi:10.1029/2004JB003209.

Petersen, Mark D. and Steven G. Wesnousky (1994). Fault slip rates and earthquake histories for active faults in southern California, *Bulletin of the Seismological Society of America* **84**, No. 5, 1608-1649.

Plesch, A., Shaw, J. & SCEC USR focus group members (2004). Community Fault Model (CFM) and Community Block Model (CBM) for Southern California, SCEC Annual Meeting, Palm Springs, CA.

Salyards, S. L., K. E. Sieh, and J. Kirshvinck (1992). Paleomagnetic measurement of non-brittle coseismic deformation across the San Andreas fault at Pallett Creek, *Journal of Geophysical Research* **97**, 12457-12470.

Sieh, K.E. (1984). Lateral offsets and revised dates of large prehistoric earthquakes at Pallett Creek southern California, *Journal of Geophysical Research* **89**, 7641-7670.

Sieh, Kerry E. and R. H. Jahns (1984). Holocene activity of the San Andreas at Wallace Creek, California, *Geological Society of America Bulletin* **95**, 883-896.

Southern California Earthquake Center (2003). Fault Information System, *Fault Activity Database*. http://epicenter.usc.edu/searchById/searchByFault.do (1 Sep. 2005).

Southern California Earthquake Center (2005). *LA3D* (v. 1.0.3). http://epicenter.usc.edu/la3d/ (1 Aug. 2005).

Wesnousky, Steven G. (1986). Earthquakes, Quaternary faults, and seismic hazard in California, *Journal of Geophysical Research* **91**, 12587-12631.

Appendix A: Segment File

We converted the CFM and CBM fault segments from UTM 11 coordinates to latitude and longitude coordinates. Segments that have been imported from the surface trace of the CFM are labeled as *faultname*_trace_*faultnumber*. We have preserved the fault names used in the CFM. The fault numbers were assigned when the fault segments were imported from the CFM and converted from UTM 11 to latitude and longitude coordinates.

The CFM faults in UTM 11 coordinates contain a series of vertices delineating the trace of each fault. We first converted each vertex to latitude and longitude coordinates. Then, we separated each fault into sequentially numbered, individual fault segments with endpoints given by the vertices. However, because *blocks_sp1* rounds coordinates to the nearest .001 degree, the high detail of the CFM faults often produced fault segments with lengths of 0. We first eliminated all of these zero length segments. Then, we merged adjacent fault segments that were very small (less than 0.005° total length) or had similar slopes upon graphic inspection. When segments with the same fault name were merged, the name of the segment with the lower number was kept. For example, channel_islands_trace_21, channel_islands_trace_22, and channel_islands_trace_23 were merged into one segment, using the northernmost endpoint from channel_islands_trace_21 and the southernmost endpoint from channel_islands_trace_23. The merged segment is listed in our file as channel_islands_trace_21. Segments for CFM faults without "trace" in the name (*e.g.* channel_islands_00) connect the CFM faults with surrounding faults to create a closed block geometry.

CBM faults are labeled as *faultname_number*. Faults were imported from the CBM in the same manner, but the CBM faults are less detailed and thus did not need to be merged.

The following pages list all 967 faults in our segment file:

Name	longitude1	latitude1	longitude2	latitude2	dip	locking depth
avawatz	243.386	35.6	243.692	35.183	45	15 (km)
bigbend1	243.637	34.161	243.751	33.804	90	5
bigbend2	243.751	33.804	243.76	33.775	90	15
blackwater1	242.399	35.47	242.528	35.244	90	5
blackwater2	242.528	35.244	242.602	35.212	90	5
blackwater3	242.602	35.212	242.941	34.97	90	5
blackwater4	242.941	34.97	243.084	34.873	90	5
BradVenturaSplit01a	240.583	34.422	240.617	34.341	90	10
BradVenturaSplit01b	240.617	34.341	240.661	34.237	90	10
calico1	243.084	34.873	243.259	34.708	90	15
calico2	243.259	34.708	243.421	34.576	90	15
calico3	243.421	34.576	243.466	34.529	90	15
calicoblackwater1bb	243.572	34.292	243.637	34.161	90	5
cbmeasternmost_03	243.608	35.596	244.224	35.021	90	15
cbmeasternmost_04b	244.224	35.021	244.523	34.738	90	15
cbmeasternmost_05	244.123	34.443	244.523	34.738	90	15
cbmeastofcalicoblackwater_13	244	34.14	244.123	34.443	90	15
cbmsouthernmost_01	244	34.14	244.293	33.347	90	15
channel_islands_00	240.707	33.955	240.74	33.984	90	15
channel_islands_trace_01	240.624	33.936	240.707	33.955	90	15
channel_islands_trace_02	240.609	33.93	240.624	33.936	90	15
channel_islands_trace_03	240.59	33.926	240.609	33.93	90	15
channel_islands_trace_04	240.57	33.927	240.59	33.926	90	15
channel_islands_trace_05	240.553	33.923	240.57	33.927	90	15
channel_islands_trace_06	240.504	33.917	240.553	33.923	90	15
channel_islands_trace_08	240.48	33.917	240.504	33.917	90	15
channel_islands_trace_09	240.458	33.915	240.48	33.917	90	15
channel_islands_trace_10	240.445	33.915	240.458	33.915	90	15
channel_islands_trace_11	240.42	33.907	240.445	33.915	90	15
channel_islands_trace_12	240.409	33.9	240.42	33.907	90	15
channel_islands_trace_13	240.381	33.898	240.409	33.9	90	15
channel_islands_trace_14	240.337	33.89	240.381	33.898	90	15
channel_islands_trace_16	240.318	33.881	240.337	33.89	90	15
channel_islands_trace_17	240.302	33.875	240.318	33.881	90	15
channel_islands_trace_18	240.29	33.872	240.302	33.875	90	15
channel_islands_trace_19	240.279	33.871	240.29	33.872	90	15
channel_islands_trace_20	240.245	33.874	240.279	33.871	90	15
channel_islands_trace_21	240.196	33.87	240.245	33.874	90	15
channel_islands_trace_24	240.156	33.874	240.196	33.87	90	15
channel_islands_trace_25	240.134	33.883	240.156	33.874	90	15
channel_islands_trace_26	240.119	33.886	240.134	33.883	90	15
channel_islands_trace_27	240.097	33.898	240.119	33.886	90	15
channel_islands_trace_28	240.089	33.903	240.097	33.898	90	15
chino_glenivy_connect	242.434	33.824	242.441	33.818	45	15
chino_trace_01	242.412	33.846	242.434	33.824	45	15
chino_trace_03	242.403	33.854	242.412	33.846	45	15
chino_trace_04	242.396	33.863	242.403	33.854	45	15
chino_trace_05	242.387	33.872	242.396	33.863	45	15
chino_trace_06	242.371	33.886	242.387	33.872	45	15
chino_trace_07	242.352	33.909	242.371	33.886	45	15
chino_trace_09	242.312	33.949	242.352	33.909	45	15

Name	longitude1	latitude1	longitude2	latitude2	dip	locking depth
chino_trace_12	242.3	33.958	242.312	33.949	45	15
chino_trace_13	242.292	33.967	242.3	33.958	45	15
chino_trace_14	242.277	34.008	242.292	33.967	45	15
chino_trace_15	242.255	34.033	242.277	34.008	45	15
chino_cucamonga_connect	242.255	34.033	242.272	34.125	90	15
coastal_ranges_split	240.478	35.027	240.583	34.422	90	15
coronadobanks_00	242.757	32.46	243.141	31.575	115	15
coronado_banks_trace_02	242.75	32.479	242.757	32.46	115	15
coronado_banks_trace_03	242.734	32.497	242.75	32.479	115	15
coronado_banks_trace_04	242.685	32.596	242.734	32.497	115	15
coronado_banks_trace_11	242.676	32.601	242.685	32.596	115	15
coronado_banks_trace_12	242.656	32.626	242.676	32.601	115	15
coronado_banks_trace_15	242.65	32.628	242.656	32.626	115	15
coronado_banks_trace_16	242.635	32.64	242.65	32.628	115	15
coronado_banks_trace_17	242.627	32.652	242.635	32.64	115	15
coronado_banks_trace_18	242.587	32.68	242.627	32.652	115	15
coronado_banks_trace_20	242.572	32.707	242.587	32.68	115	15
coronado_banks_trace_22	242.562	32.734	242.572	32.707	115	15
coronado_banks_trace_25	242.556	32.74	242.562	32.734	115	15
coronado_banks_trace_26	242.533	32.754	242.556	32.74	115	15
coronado_banks_trace_28	242.523	32.769	242.533	32.754	115	15
coronado_banks_trace_29	242.521	32.777	242.523	32.769	115	15
coronado_banks_trace_30	242.494	32.81	242.521	32.777	115	15
coronado_banks_trace_33	242.494	32.81	242.495	32.821	115	15
coronado_banks_trace_34	242.48	32.867	242.495	32.821	115	15
coronado_banks_trace_36	242.46	32.895	242.48	32.867	115	15
coronado_banks_trace_38	242.392	32.949	242.46	32.895	115	15
coyotelake1	242.941	34.97	243.225	35.148	90	10
coyotelake2	243.225	35.148	243.331	35.153	90	10
coyotelake3	243.331	35.153	243.447	35.148	90	10
coyotelake4	243.447	35.148	243.692	35.183	90	10
crude_jdf1	230.593	47.95	235.278	40.845	90	15
cucamonga_trace_01	242.491	34.174	242.566	34.184	130	15
cucamonga_trace_02	242.441	34.174	242.491	34.174	130	15
cucamonga_trace_03	242.4	34.167	242.441	34.174	130	15
cucamonga_trace_04	242.372	34.164	242.4	34.167	130	15
cucamonga_trace_05	242.272	34.125	242.372	34.164	130	15
cucamonga_connect	242.566	34.184	242.605	34.178	130	15
cucamongaextension	242.605	34.178	242.663	34.207	130	15
deathvalley4	240.58	39	242.06	37.483	90	10
death_valley_00	243.11	36.516	243.122	36.539	90	15
death_valley_trace_03	243.11	36.516	243.123	36.499	90	15
death_valley_trace_05	243.123	36.499	243.142	36.481	90	15
death_valley_trace_07	243.142	36.481	243.156	36.447	90	15
death_valley_trace_09	243.156	36.447	243.16	36.426	90	15
death_valley_trace_11	243.16	36.426	243.167	36.409	90	15
death_valley_trace_12	243.167	36.409	243.171	36.406	90	15
death_valley_trace_13	243.171	36.406	243.179	36.386	90	15
death_valley_trace_15	243.179	36.386	243.204	36.358	90	15
death_valley_trace_18	243.204	36.358	243.21	36.341	90	15
death_valley_trace_19	243.21	36.341	243.214	36.336	90	15

Name	longitude1	latitude1	longitude2	latitude2	dip	locking depth
death_valley_trace_20	243.214	36.336	243.224	36.318	90	15
death_valley_trace_22	243.224	36.31	243.224	36.318	90	15
death_valley_trace_23	243.224	36.31	243.234	36.285	90	15
death_valley_trace_25	243.234	36.273	243.234	36.285	90	15
death_valley_trace_26	243.23	36.263	243.234	36.273	90	15
death_valley_trace_27	243.23	36.263	243.232	36.254	90	15
death_valley_trace_28	243.232	36.254	243.236	36.249	90	15
death_valley_trace_29	243.236	36.249	243.241	36.23	90	15
death_valley_trace_31	243.239	36.219	243.241	36.23	90	15
death_valley_trace_32	243.239	36.219	243.245	36.196	90	15
death_valley_trace_33	243.245	36.196	243.246	36.174	90	15
death_valley_trace_35	243.242	36.153	243.246	36.174	90	15
death_valley_trace_36	243.242	36.153	243.244	36.145	90	15
death_valley_trace_37	243.244	36.145	243.275	36.104	90	15
death_valley_trace_41	243.275	36.104	243.279	36.092	90	15
death_valley_trace_42	243.246	36.06	243.279	36.092	90	15
death_valley_trace_43	243.243	36.054	243.246	36.06	90	15
death_valley_trace_45	243.243	36.054	243.276	36.004	90	15
death_valley_trace_48	243.276	36.004	243.278	35.985	90	15
death_valley_trace_49	243.278	35.985	243.289	35.967	90	15
death_valley_trace_51	243.287	35.961	243.289	35.967	90	15
death_valley_trace_52	243.287	35.961	243.289	35.955	90	15
death_valley_trace_53	243.289	35.955	243.295	35.948	90	15
death_valley_trace_54	243.291	35.925	243.295	35.948	90	15
death_valley_trace_56	243.291	35.925	243.311	35.907	90	15
death_valley_trace_58	243.311	35.907	243.318	35.895	90	15
death_valley_trace_60	243.318	35.895	243.336	35.877	90	15
death_valley_trace_63	243.336	35.877	243.344	35.877	90	15
death_valley_trace_64	243.344	35.877	243.384	35.846	90	15
death_valley_trace_66	243.384	35.846	243.399	35.791	90	15
death_valley_trace_69	243.399	35.791	243.432	35.752	90	15
death_valley_trace_72	243.432	35.752	243.445	35.724	90	15
death_valley_trace_77	243.445	35.724	243.484	35.703	90	15
death_valley_trace_78	243.484	35.703	243.541	35.648	90	15
death_valley_trace_81	243.541	35.648	243.551	35.627	90	15
death_valley_trace_86	243.551	35.627	243.57	35.617	90	15
death_valley_trace_87	243.57	35.617	243.574	35.613	90	15
death_valley_trace_88	243.574	35.613	243.601	35.603	90	15
death_valley_91	243.601	35.603	243.608	35.596	90	15
deepspringsvalley1	241.946	37.15	242.06	37.483	90	10
Eastern_closure1	216.76	55.69	325.661	58.239	90	15
Eastern_closure2	274.413	-13.347	325.661	58.239	90	15
Eastern_closure3	260.639	5.079	274.413	-13.347	90	15
eastnorthfrontalzone1	243.196	34.338	243.256	34.333	45	15
eastnorthfrontalzone2	243.256	34.333	243.29	34.346	45	15
eastnorthfrontalzone3	243.29	34.346	243.33	34.332	45	15
eastnorthfrontalzone4	243.33	34.332	243.357	34.34	45	15
eastnorthfrontalzone5	243.357	34.34	243.411	34.321	45	15
eastnorthfrontalzone6	243.411	34.321	243.461	34.319	45	15
eastnorthfrontalzone7	243.461	34.319	243.572	34.292	45	15
coyote_connect	244.117	32.729	245.066	32.154	90	15

Name	longitude1	latitude1	longitude2	latitude2	dip	locking depth
coyotemountain_00	243.959	32.787	244.117	32.729	90	15
coyote_mntn_elsinore_trace_01	243.914	32.807	243.959	32.787	90	15
coyote_mntn_elsinore_trace_03	243.901	32.816	243.914	32.807	90	15
coyote_mntn_elsinore_trace_04	243.866	32.83	243.901	32.816	90	15
coyote_mntn_elsinore_trace_05	243.822	32.839	243.866	32.83	90	15
coyote_mntn_elsinore_trace_10	243.807	32.848	243.822	32.839	90	15
coyote_mntn_elsinore_trace_11	243.782	32.868	243.807	32.848	90	15
coyote_mntn_elsinore_trace_12	243.755	32.891	243.782	32.868	90	15
coyote_mntn_elsinore_trace_13	243.714	32.949	243.755	32.891	90	15
coyote_mntn_elsinore_trace_16	243.708	32.951	243.714	32.949	90	15
coyote_mntn_elsinore_trace_17	243.69	32.965	243.708	32.951	90	15
coyote_mntn_elsinore_trace_18	243.687	32.969	243.69	32.965	90	15
coyote_mntn_elsinore_trace_19	243.6	32.992	243.687	32.969	90	15
coyote_mntn_elsinore_trace_20	243.588	32.993	243.6	32.992	90	15
coyote_mntn_elsinore_trace_21	243.577	32.992	243.588	32.993	90	15
coyote_mntn_elsinore_trace_22	243.556	32.988	243.577	32.992	90	15
julian_elsinore_00	243.543	32.992	243.556	32.988	90	15
julian_elsinore_trace_08	243.528	33.005	243.543	32.992	90	15
julian_elsinore_trace_09	243.496	33.026	243.528	33.005	90	15
julian_elsinore_trace_10	243.485	33.038	243.496	33.026	90	15
julian_elsinore_trace_11	243.372	33.124	243.485	33.038	90	15
julian_elsinore_trace_17	243.354	33.14	243.372	33.124	90	15
julian_elsinore_trace_18	243.326	33.16	243.354	33.14	90	15
julian_elsinore_trace_19	243.31	33.169	243.326	33.16	90	15
julian_elsinore_trace_20	243.268	33.204	243.31	33.169	90	15
julian_elsinore_trace_21	243.184	33.266	243.268	33.204	90	15
julian_elsinore_trace_24	243.156	33.281	243.184	33.266	90	15
julian_elsinore_trace_25	243.13	33.29	243.156	33.281	90	15
julian_elsinore_trace_26	242.998	33.357	243.13	33.29	90	15
julian_elsinore_trace_31	242.972	33.376	242.998	33.357	90	15
julian_elsinore_trace_32	242.969	33.386	242.972	33.376	90	15
julian_temecula_connect	242.913	33.436	242.969	33.386	90	15
temecula_elsinore_trace_01	242.804	33.519	242.913	33.436	90	15
temecula_elsinore_trace_06	242.762	33.571	242.804	33.519	90	15
furnace_creek_trace_01	243.119	36.551	243.122	36.539	90	15
furnace_creek_trace_02	243.108	36.563	243.119	36.551	90	15
furnace_creek_trace_04	243.095	36.564	243.108	36.563	90	15
furnace_creek_trace_05	243.056	36.595	243.095	36.564	90	15
furnace_creek_trace_07	243.05	36.598	243.056	36.595	90	15
furnace_creek_trace_08	243.012	36.625	243.05	36.598	90	15
furnace_creek_trace_10	243.005	36.635	243.012	36.625	90	15
furnace_creek_trace_12	242.844	36.76	243.005	36.635	90	15
furnace_creek_trace_21	242.82	36.799	242.844	36.76	90	15
furnace_creek_trace_23	242.791	36.827	242.82	36.799	90	15
furnace_creek_trace_26	242.785	36.84	242.791	36.827	90	15
furnace_creek_trace_27	242.768	36.855	242.785	36.84	90	15
furnace_creek_trace_29	242.758	36.869	242.768	36.855	90	15
furnace_creek_trace_31	242.755	36.878	242.758	36.869	90	15
furnace_creek_trace_32	242.717	36.914	242.755	36.878	90	15
furnace_creek_trace_34	242.714	36.924	242.717	36.914	90	15
furnace_creek_trace_35	242.687	36.96	242.714	36.924	90	15

Name	longitude1	latitude1	longitude2	latitude2	dip	locking depth
furnace_creek_trace_38	242.666	36.974	242.687	36.96	90	15
furnace_creek_trace_39	242.652	36.997	242.666	36.974	90	15
furnace_creek_trace_41	242.624	37.018	242.652	36.997	90	15
furnace_creek_trace_42	242.62	37.026	242.624	37.018	90	15
furnace_creek_trace_43	242.588	37.059	242.62	37.026	90	15
furnace_creek_trace_46	242.558	37.08	242.588	37.059	90	15
furnace_creek_trace_48	242.348	37.296	242.558	37.08	90	15
furnace_creek_connect	242.06	37.483	242.348	37.296	90	15
garlock01	241.072	34.818	241.171	34.855	90	25
garlock02	241.171	34.855	241.282	34.911	90	15
garlock03	241.282	34.911	241.528	34.998	90	15
garlock04	241.528	34.998	241.653	35.081	90	15
garlock05	241.653	35.081	241.91	35.209	90	15
garlock06	241.91	35.209	241.986	35.271	90	15
garlock07	241.978	35.285	241.986	35.271	90	15
garlock08	241.978	35.285	241.991	35.292	90	15
garlock09	241.991	35.292	242.187	35.398	90	15
garlock10	242.187	35.398	242.286	35.433	90	15
garlock11	242.286	35.433	242.399	35.47	90	15
garlock12	242.399	35.47	242.448	35.486	90	15
garlock13	242.448	35.486	242.706	35.543	90	15
garlock15	242.706	35.543	242.861	35.585	90	15
garlock17	242.861	35.585	242.898	35.591	90	15
garlock18	242.898	35.591	242.987	35.604	90	15
garlock19	242.987	35.604	243.118	35.602	90	15
garlock20	243.118	35.602	243.386	35.6	90	15
garlock21	243.386	35.6	243.608	35.596	90	15
glenivy_temecula_connect	242.73	33.64	242.762	33.571	90	15
glen_ivy_trace_01	242.617	33.698	242.73	33.64	90	15
glen_ivy_trace_06	242.483	33.793	242.617	33.698	90	15
glen_ivy_trace_12b	242.452	33.815	242.483	33.793	45	15
glen_ivy_trace_13	242.441	33.818	242.452	33.815	45	15
goldstone1	242.898	35.591	243.075	35.455	90	10
goldstone2	243.075	35.455	243.331	35.153	90	10
helendale1	242.672	34.789	242.894	34.606	90	10
helendale2	242.894	34.606	242.897	34.601	90	10
helendale3	242.897	34.601	242.936	34.541	90	10
helendale4	242.936	34.541	243.055	34.443	90	10
helendale5	243.055	34.443	243.143	34.377	90	10
helendale6	243.143	34.377	243.148	34.371	90	10
helendale7	243.148	34.371	243.196	34.338	45	10
hidalgo1	243.466	34.529	243.473	34.488	90	10
hidalgo2	243.473	34.488	243.515	34.45	90	10
hidalgo3	243.515	34.45	243.536	34.403	90	10
hidalgo4	243.536	34.403	243.562	34.37	90	10
hidalgo5	243.562	34.37	243.572	34.292	90	10
hosgri_san_simeon_00	239.313	34.606	239.335	34.565	115	15
hosgri_san_simeon_trace_01	239.308	34.709	239.313	34.606	115	15
hosgri_san_simeon_trace_04	239.297	34.741	239.308	34.709	115	15
hosgri_san_simeon_trace_05	239.267	34.797	239.297	34.741	115	15
hosgri_san_simeon_trace_07	239.267	34.797	239.268	34.817	65	15

Name	longitude1	latitude1	longitude2	latitude2	dip	locking depth
hosgri_san_simeon_trace_08	239.234	34.895	239.268	34.817	115	15
hosgri_san_simeon_trace_10	239.205	34.936	239.234	34.895	115	15
hosgri_san_simeon_trace_11	239.195	34.977	239.205	34.936	115	15
hosgri_san_simeon_trace_12	239.166	35.049	239.195	34.977	115	15
hosgri_san_simeon_trace_14	239.121	35.145	239.166	35.049	115	15
hosgri_san_simeon_trace_17	239.084	35.194	239.121	35.145	115	15
hosgri_san_simeon_trace_19	239.006	35.332	239.084	35.194	115	15
hosgri_san_simeon_trace_23	238.998	35.356	239.006	35.332	115	15
hosgri_san_simeon_trace_24	238.954	35.423	238.998	35.356	115	15
hosgri_san_simeon_trace_26	238.878	35.558	238.954	35.423	115	15
hosgri_san_simeon_trace_29	238.805	35.654	238.878	35.558	115	15
hosgri_san_simeon_trace_31	238.714	35.746	238.805	35.654	115	15
hosgri_san_simeon_trace_33	238.681	35.77	238.714	35.746	115	15
hosgri_san_simeon_trace_34	238.635	35.794	238.681	35.77	115	15
hosgri_san_simeon_trace_35	238.506	35.896	238.635	35.794	115	15
hosgri_san_simeon_trace_38	238.483	35.931	238.506	35.896	115	15
hosgri_san_simeon_trace_39	238.439	35.97	238.483	35.931	115	15
hosgri_san_simeon_trace_40	238.273	36.148	238.439	35.97	115	15
hosgrisansimeon_41	238.131	36.359	238.273	36.148	115	15
hunter_mountain_00	242.525	36.498	242.583	36.456	90	15
hunter_mountain_trace_01	242.52	36.498	242.525	36.498	90	15
hunter_mountain_trace_02	242.503	36.505	242.52	36.498	90	15
hunter_mountain_trace_04	242.497	36.511	242.503	36.505	90	15
hunter_mountain_trace_05	242.481	36.518	242.497	36.511	90	15
hunter_mountain_trace_06	242.47	36.525	242.481	36.518	90	15
hunter_mountain_trace_07	242.432	36.542	242.47	36.525	90	15
hunter_mountain_trace_10	242.413	36.56	242.432	36.542	90	15
hunter_mountain_trace_11	242.388	36.574	242.413	36.56	90	15
hunter_mountain_trace_13	242.342	36.615	242.388	36.574	90	15
hunter_mountain_trace_15	242.294	36.636	242.342	36.615	90	15
hunter_mountain_trace_18	242.252	36.645	242.294	36.636	90	15
hunter_mountain_trace_20	242.18	36.674	242.252	36.645	90	15
hunter_mountain_trace_24	242.174	36.692	242.18	36.674	90	15
hunter_mountain_trace_25	242.164	36.696	242.174	36.692	90	15
hunter_mountain_trace_26	242.142	36.726	242.164	36.696	90	15
hunter_mountain_trace_28	242.139	36.739	242.142	36.726	90	15
hunter_mountain_trace_29	242.113	36.759	242.139	36.739	90	15
hunter_mountain_trace_31	242.103	36.783	242.113	36.759	90	15
hunter_mountain_trace_33	242.1	36.803	242.103	36.783	90	15
hunter_mountain_trace_35	242.09	36.815	242.1	36.803	90	15
hunter_mountain_trace_36	242.088	36.822	242.09	36.815	90	15
hunter_mountain_trace_37	242.082	36.829	242.088	36.822	90	15
hunter_mountain_trace_38	242.048	36.925	242.082	36.829	90	15
little_lake_00	242.213	35.781	242.448	35.486	90	15
little_lake_trace_01b	242.146	35.87	242.213	35.781	90	15
little_lake_trace_02	242.14	35.88	242.146	35.87	90	15
little_lake_trace_03	242.119	35.897	242.14	35.88	90	15
little_lake_trace_04	242.114	35.907	242.119	35.897	90	15
little_lake_trace_05	242.099	35.926	242.114	35.907	90	15
little_lake_trace_06	242.093	35.938	242.099	35.926	90	15
littlelake_sierranevada_connector	242.065	35.949	242.093	35.938	90	15

Name	longitude1	latitude1	longitude2	latitude2	dip	locking depth
lockhart1	241.991	35.292	242.224	35.217	90	10
lockhart2	242.224	35.217	242.4	35.122	90	10
southlockhart1	242.4	35.122	242.503	35.045	90	15
southlockhart2	242.503	35.045	242.672	34.789	90	15
ludlow1	243.692	35.183	243.818	35.067	90	10
ludlow2	243.749	34.961	243.818	35.067	90	10
ludlow3	243.749	34.961	243.797	34.908	90	10
ludlow4	243.783	34.825	243.797	34.908	90	10
ludlow5	243.783	34.825	243.811	34.785	90	10
ludlow6	243.811	34.785	243.839	34.707	90	10
ludlow7	243.839	34.707	244.123	34.443	90	10
Nevada01	244.224	35.021	246.689	37.971	90	10
Nevada02	246.603	41.89	246.689	37.971	90	10
Nevada03	235.958	43.583	246.603	41.89	90	10
new_pacific	240.445	33.915	241.192	33.288	90	15
newport1b_new	242.805	32.702	244.239	31.325	90	15
newport_inglewood_trace_01	242.803	32.708	242.805	32.702	90	15
newport_inglewood_trace_07	242.8	32.715	242.803	32.708	90	15
newport_inglewood_trace_15	242.798	32.718	242.8	32.715	90	15
newport_inglewood_trace_18	242.718	32.91	242.798	32.718	90	15
newport_inglewood_trace_21	242.714	32.923	242.718	32.91	90	15
newport_inglewood_trace_38	242.663	33.066	242.714	32.923	90	15
newport_inglewood_trace_40	242.658	33.074	242.663	33.066	90	15
newport_inglewood_trace_64	242.655	33.077	242.658	33.074	90	15
newport_inglewood_trace_70	242.585	33.179	242.655	33.077	90	15
newport_inglewood_trace_71	242.477	33.291	242.585	33.179	90	15
newport_inglewood_trace_121	242.476	33.293	242.477	33.291	90	15
newport_inglewood_trace_123	242.401	33.371	242.476	33.293	90	15
newport_inglewood_trace_141	242.392	33.377	242.401	33.371	90	15
newport_inglewood_trace_148	242.165	33.554	242.392	33.377	90	15
newport_inglewood_trace_152b	242.005	33.677	242.165	33.554	90	15
newport_inglewood_trace_154	241.957	33.703	242.005	33.677	90	15
newport_inglewood_trace_160	241.952	33.709	241.957	33.703	90	15
newport_inglewood_trace_161	241.945	33.713	241.952	33.709	90	15
newport_inglewood_trace_162	241.939	33.721	241.945	33.713	90	15
newport_inglewood_trace_163	241.917	33.743	241.939	33.721	90	15
newport_inglewood_trace_170	241.889	33.763	241.917	33.743	90	15
newport_inglewood_trace_174	241.884	33.767	241.889	33.763	90	15
newport_inglewood_trace_177	241.852	33.783	241.884	33.767	90	15
newport_inglewood_trace_181	241.845	33.788	241.852	33.783	90	15
newport_inglewood_trace_182	241.838	33.794	241.845	33.788	90	15
newport_inglewood_trace_183	241.82	33.804	241.838	33.794	90	15
newport_inglewood_trace_185	241.801	33.825	241.82	33.804	90	15
newport_inglewood_trace_189	241.797	33.828	241.801	33.825	90	15
newport_inglewood_trace_190	241.787	33.832	241.797	33.828	90	15
newport_inglewood_trace_204	241.768	33.844	241.787	33.832	90	15
newport_inglewood_trace_205	241.761	33.852	241.768	33.844	90	15
newport_inglewood_trace_208	241.753	33.866	241.761	33.852	90	15
newport_inglewood_trace_212	241.747	33.874	241.753	33.866	90	15
newport_inglewood_trace_214	241.745	33.878	241.747	33.874	90	15
newport_inglewood_trace_215	241.744	33.881	241.745	33.878	90	15

Name	longitude1	latitude1	longitude2	latitude2	dip	locking depth
newport_inglewood_trace_216	241.736	33.885	241.744	33.881	90	15
newport_inglewood_trace_217	241.731	33.896	241.736	33.885	90	15
newport_inglewood_trace_220	241.73	33.9	241.731	33.896	90	15
newport_inglewood_trace_221	241.722	33.919	241.73	33.9	90	15
newport_inglewood_trace_226	241.712	33.911	241.722	33.919	90	15
newport_inglewood_trace_227	241.706	33.923	241.712	33.911	90	15
newport_inglewood_trace_238	241.702	33.923	241.706	33.923	90	15
newport_inglewood_trace_240	241.7	33.927	241.702	33.923	90	15
newport_inglewood_trace_242	241.696	33.931	241.7	33.927	90	15
newport_inglewood_trace_247	241.681	33.934	241.696	33.931	90	15
newport_inglewood_trace_248	241.674	33.944	241.681	33.934	90	15
newport_inglewood_trace_256	241.649	33.995	241.674	33.944	90	15
newport_inglewood_trace_305	241.639	33.994	241.649	33.995	90	15
newport_inglewood_trace_312	241.617	34.033	241.639	33.994	90	15
newport_inglewood_trace_330	241.613	34.042	241.617	34.033	90	15
newport_inglewood_333	241.587	34.051	241.613	34.042	90	15
oakridge_on_01	241.095	34.383	241.125	34.395	45	15
oakridge_on_trace_09	241.087	34.382	241.095	34.383	45	15
oakridge_on_trace_10	241.077	34.37	241.087	34.382	45	15
oakridge_on_trace_12	241.067	34.371	241.077	34.37	45	15
oakridge_on_trace_13	241.048	34.361	241.067	34.371	45	15
oakridge_on_trace_16	241.029	34.355	241.048	34.361	45	15
oakridge_on_trace_18	241.015	34.347	241.029	34.355	45	15
oakridge_on_trace_20	240.992	34.352	241.015	34.347	45	15
oakridge_on_trace_22	240.975	34.353	240.992	34.352	45	15
oakridge_on_trace_24	240.957	34.351	240.975	34.353	45	15
oakridge_on_trace_26	240.938	34.34	240.957	34.351	45	15
oakridge_on_trace_29	240.926	34.332	240.938	34.34	45	15
oakridge_on_trace_31	240.907	34.316	240.926	34.332	45	15
oakridge_on_trace_33	240.801	34.264	240.907	34.316	45	15
oakridge_on_trace_43	240.781	34.262	240.801	34.264	45	15
oakridge_on_trace_45	240.767	34.258	240.781	34.262	45	15
oakridge_on_trace_47	240.747	34.257	240.767	34.258	45	15
oakridge_on_50	240.661	34.237	240.747	34.257	45	15
oceanside_00	242.392	32.949	242.393	32.952	90	15
oceanside_trace_242	242.393	32.952	242.393	32.956	90	15
oceanside_trace_243	242.393	32.956	242.399	32.967	90	15
oceanside_trace_247	242.399	32.967	242.402	32.98	90	15
oceanside_trace_250	242.393	33.003	242.402	32.98	90	15
oceanside_trace_254	242.389	33.018	242.393	33.003	90	15
oceanside_trace_260	242.385	33.027	242.389	33.018	90	15
oceanside_trace_263	242.385	33.027	242.385	33.04	90	15
oceanside_trace_270	242.384	33.042	242.385	33.04	90	15
oceanside_trace_271	242.384	33.042	242.386	33.051	90	15
oceanside_trace_275	242.385	33.053	242.386	33.051	90	15
oceanside_trace_276	242.385	33.053	242.385	33.057	90	15
oceanside_trace_277	242.374	33.06	242.385	33.057	90	15
oceanside_trace_280	242.371	33.062	242.374	33.06	90	15
oceanside_trace_282	242.361	33.066	242.371	33.062	90	15
oceanside_trace_287	242.359	33.066	242.361	33.066	90	15
oceanside_trace_288	242.356	33.068	242.359	33.066	90	15

Name	longitude1	latitude1	longitude2	latitude2	dip	locking depth
oceanside_trace_290	242.352	33.07	242.356	33.068	90	15
oceanside_trace_291	242.349	33.073	242.352	33.07	90	15
oceanside_trace_294	242.345	33.076	242.349	33.073	90	15
oceanside_trace_297	242.342	33.082	242.345	33.076	90	15
oceanside_trace_299	242.34	33.084	242.342	33.082	90	15
oceanside_trace_300	242.339	33.087	242.34	33.084	90	15
oceanside_trace_301	242.336	33.091	242.339	33.087	90	15
oceanside_trace_304	242.336	33.091	242.336	33.093	90	15
oceanside_trace_305	242.333	33.098	242.336	33.093	90	15
oceanside_trace_307	242.333	33.098	242.333	33.1	90	15
oceanside_trace_308	242.332	33.102	242.333	33.1	90	15
oceanside_trace_309	242.332	33.102	242.332	33.104	90	15
oceanside_trace_311	242.331	33.108	242.332	33.104	90	15
oceanside_trace_312	242.318	33.16	242.331	33.108	90	15
oceanside_trace_324	242.311	33.165	242.318	33.16	90	15
oceanside_trace_327	242.307	33.166	242.311	33.165	90	15
oceanside_trace_329	242.305	33.169	242.307	33.166	90	15
oceanside_trace_330	242.305	33.169	242.305	33.172	90	15
oceanside_trace_331	242.305	33.172	242.308	33.177	90	15
oceanside_trace_333	242.308	33.177	242.308	33.179	90	15
oceanside_trace_334	242.308	33.179	242.31	33.182	90	15
oceanside_trace_335	242.288	33.219	242.31	33.182	90	15
oceanside_trace_338	242.274	33.227	242.288	33.219	90	15
oceanside_trace_342	242.271	33.231	242.274	33.227	90	15
oceanside_trace_343	242.267	33.24	242.271	33.231	90	15
oceanside_trace_344	242.257	33.241	242.267	33.24	90	15
oceanside_trace_348	242.254	33.246	242.257	33.241	90	15
oceanside_trace_349	242.252	33.246	242.254	33.246	90	15
oceanside_trace_350	242.251	33.248	242.252	33.246	90	15
oceanside_trace_352	242.251	33.248	242.252	33.25	90	15
oceanside_trace_353	242.252	33.25	242.254	33.265	90	15
oceanside_trace_356	242.251	33.272	242.254	33.265	90	15
oceanside_trace_360	242.251	33.272	242.252	33.275	90	15
oceanside_trace_362	242.25	33.279	242.252	33.275	90	15
oceanside_trace_365	242.25	33.279	242.252	33.285	90	15
oceanside_trace_370	242.252	33.285	242.252	33.292	90	15
oceanside_trace_374	242.251	33.294	242.252	33.292	90	15
oceanside_trace_375	242.251	33.294	242.251	33.301	90	15
oceanside_trace_379	242.251	33.301	242.251	33.303	90	15
oceanside_trace_381	242.25	33.311	242.251	33.303	90	15
oceanside_trace_385	242.249	33.312	242.25	33.311	90	15
oceanside_trace_386	242.249	33.312	242.25	33.315	90	15
oceanside_trace_389	242.25	33.315	242.25	33.317	90	15
oceanside_trace_390	242.249	33.326	242.25	33.317	90	15
oceanside_trace_397	242.249	33.326	242.253	33.333	90	15
oceanside_trace_401	242.252	33.339	242.253	33.333	90	15
oceanside_trace_406	242.252	33.339	242.253	33.344	90	15
oceanside_trace_408	242.253	33.344	242.253	33.35	90	15
oceanside_trace_410	242.252	33.353	242.253	33.35	90	15
oceanside_trace_411	242.252	33.353	242.252	33.356	90	15
oceanside_trace_413	242.25	33.361	242.252	33.356	90	15

Name	longitude1	latitude1	longitude2	latitude2	dip	locking depth
oceanside_trace_415	242.249	33.366	242.25	33.361	90	15
oceanside_trace_417	242.242	33.379	242.249	33.366	90	15
oceanside_trace_423	242.233	33.392	242.242	33.379	90	15
oceanside_trace_430	242.227	33.397	242.233	33.392	90	15
oceanside_trace_433	242.226	33.399	242.227	33.397	90	15
oceanside_trace_434	242.221	33.405	242.226	33.399	90	15
oceanside_trace_438	242.212	33.418	242.221	33.405	90	15
oceanside_trace_444	242.211	33.422	242.212	33.418	90	15
oceanside_trace_445	242.209	33.424	242.211	33.422	90	15
oceanside_trace_446	242.208	33.427	242.209	33.424	90	15
oceanside_trace_447	242.191	33.456	242.208	33.427	90	15
oceanside_trace_455	242.19	33.46	242.191	33.456	90	15
oceanside_trace_456	242.187	33.467	242.19	33.46	90	15
oceanside_trace_459	242.182	33.481	242.187	33.467	90	15
oceanside_trace_463	242.182	33.481	242.182	33.485	90	15
oceanside_trace_464	242.18	33.493	242.182	33.485	90	15
oceanside_trace_466	242.179	33.511	242.18	33.493	90	15
oceanside_472	242.165	33.554	242.179	33.511	90	15
owensvalleynorth1a	216.76	55.69	230.593	47.95	90	15
owensvalleynorth1ba	230.593	47.95	235.958	43.583	90	15
owensvalleynorth1bb	235.958	43.583	240.58	39	90	15
owensvalleynorth2	240.58	39	241.521	37.633	90	10
owensvalleynorth3	241.521	37.633	241.671	37.236	90	10
owens_valley_trace_01	241.958	36.554	241.98	36.507	90	15
owens_valley_trace_04	241.941	36.604	241.958	36.554	90	15
owens_valley_trace_06	241.941	36.604	241.941	36.617	90	15
owens_valley_trace_07	241.936	36.63	241.941	36.617	90	15
owens_valley_trace_08	241.93	36.637	241.936	36.63	90	15
owens_valley_trace_09	241.918	36.687	241.93	36.637	90	15
owens_valley_trace_10	241.917	36.696	241.918	36.687	90	15
owens_valley_trace_11	241.9	36.734	241.917	36.696	90	15
owens_valley_trace_14	241.895	36.749	241.9	36.734	90	15
owens_valley_trace_15	241.885	36.764	241.895	36.749	90	15
owens_valley_trace_17	241.881	36.776	241.885	36.764	90	15
owens_valley_trace_18	241.871	36.794	241.881	36.776	90	15
owens_valley_trace_20	241.867	36.798	241.871	36.794	90	15
owens_valley_trace_21	241.836	36.862	241.867	36.798	90	15
owens_valley_trace_25	241.833	36.866	241.836	36.862	90	15
owens_valley_trace_26	241.829	36.876	241.833	36.866	90	15
owens_valley_trace_27	241.828	36.883	241.829	36.876	90	15
owens_valley_trace_28	241.823	36.898	241.828	36.883	90	15
owens_valley_trace_29	241.803	36.933	241.823	36.898	90	15
owens_valley_trace_30	241.8	36.955	241.803	36.933	90	15
owens_valley_trace_31	241.671	37.236	241.8	36.955	90	15
pacific4_new	242.615	31.995	243.141	31.575	90	15
pacific5	243.141	31.575	244.239	31.325	90	15
pacific6	244.239	31.325	245.328	29.522	90	15
pacific7	245.328	29.522	259.341	1.742	90	15
pacific_newa	239.335	34.565	239.403	34.334	90	15
pacific_newb	239.403	34.334	239.489	34.022	90	15
PAC_to_SAF_northern_closure1	190.538	57.203	191.871	57.592	90	15

Name	longitude1	latitude1	longitude2	latitude2	dip	locking depth
PalosVerdes_00	242.069	33.296	242.101	33.266	115	15
palos_verdes_trace_04	242.065	33.306	242.069	33.296	115	15
palos_verdes_trace_06	242.057	33.32	242.065	33.306	115	15
palos_verdes_trace_07	242.041	33.336	242.057	33.32	115	15
palos_verdes_trace_09	242.029	33.346	242.041	33.336	115	15
palos_verdes_trace_11	242.014	33.356	242.029	33.346	115	15
palos_verdes_trace_13	241.94	33.445	242.014	33.356	115	15
palos_verdes_trace_20	241.881	33.547	241.94	33.445	115	15
palos_verdes_trace_24	241.835	33.609	241.881	33.547	115	15
palos_verdes_trace_28	241.832	33.618	241.835	33.609	115	15
palos_verdes_trace_29	241.783	33.679	241.832	33.618	115	15
palos_verdes_trace_32	241.767	33.694	241.783	33.679	115	15
palos_verdes_trace_33	241.746	33.749	241.767	33.694	115	15
palos_verdes_trace_34	241.6	33.819	241.746	33.749	115	15
palos_verdes_trace_38	241.551	33.876	241.6	33.819	115	15
palos_verdes_trace_47	241.504	33.904	241.551	33.876	115	15
palos_verdes_trace_53	241.443	33.972	241.504	33.904	115	15
PalosVerdesRebuilt01_new	241.36	34.014	241.443	33.972	115	15
coronado_banks_trace_41b	242.384	32.954	242.392	32.949	115	15
coronado_banks_trace_42	242.314	33.029	242.384	32.954	115	15
coronado_banks_trace_46	242.291	33.042	242.314	33.029	115	15
coronado_banks_trace_48	242.272	33.063	242.291	33.042	115	15
coronado_banks_trace_51	242.258	33.075	242.272	33.063	115	15
coronado_banks_trace_52	242.242	33.108	242.258	33.075	115	15
coronado_banks_trace_55	242.215	33.141	242.242	33.108	115	15
coronado_banks_trace_59	242.207	33.142	242.215	33.141	115	15
coronado_banks_trace_60	242.163	33.194	242.207	33.142	115	15
coronado_banks_trace_65	242.162	33.208	242.163	33.194	115	15
coronado_banks_trace_66	242.101	33.266	242.162	33.208	115	15
panamint_valley_00	243.103	35.611	243.118	35.602	60	15
panamint_valley_trace_01	243.064	35.643	243.103	35.611	60	15
panamint_valley_trace_02	242.959	35.682	243.064	35.643	60	15
panamint_valley_trace_03	242.952	35.686	242.959	35.682	60	15
panamint_valley_trace_04	242.886	35.748	242.952	35.686	60	15
panamint_valley_trace_08	242.862	35.795	242.886	35.748	60	15
panamint_valley_trace_12	242.848	35.84	242.862	35.795	60	15
panamint_valley_trace_13	242.832	35.873	242.848	35.84	60	15
panamint_valley_trace_14	242.815	35.894	242.832	35.873	60	15
panamint_valley_trace_15	242.78	35.997	242.815	35.894	60	15
panamint_valley_trace_22	242.78	35.997	242.79	36.023	120	15
panamint_valley_trace_23	242.79	36.023	242.79	36.037	120	15
panamint_valley_trace_24	242.79	36.037	242.8	36.051	120	15
panamint_valley_trace_25	242.8	36.051	242.808	36.079	120	15
panamint_valley_trace_27	242.807	36.089	242.808	36.079	60	15
panamint_valley_trace_28	242.794	36.108	242.807	36.089	60	15
panamint_valley_trace_29	242.791	36.118	242.794	36.108	60	15
panamint_valley_trace_30	242.791	36.118	242.791	36.138	120	15
panamint_valley_trace_32	242.791	36.138	242.794	36.146	120	15
panamint_valley_trace_33	242.794	36.146	242.797	36.195	120	15
panamint_valley_trace_34	242.782	36.212	242.797	36.195	60	15
panamint_valley_trace_36	242.772	36.237	242.782	36.212	60	15

Name	longitude1	latitude1	longitude2	latitude2	dip	locking depth
panamint_valley_trace_37	242.74	36.269	242.772	36.237	60	15
panamint_valley_trace_40	242.725	36.273	242.74	36.269	60	15
panamint_valley_trace_41	242.706	36.283	242.725	36.273	60	15
panamint_valley_trace_43	242.673	36.322	242.706	36.283	60	15
panamint_valley_trace_47	242.67	36.332	242.673	36.322	60	15
panamint_valley_trace_48	242.661	36.339	242.67	36.332	60	15
panamint_valley_trace_49	242.64	36.366	242.661	36.339	60	15
panamint_valley_trace_50	242.639	36.374	242.64	36.366	60	15
panamint_valley_53	242.583	36.456	242.639	36.374	60	15
PHTGuess_new	241.733	34.115	242.009	33.82	135	15
PhtOne_new	242.301	33.774	242.483	33.793	135	15
PhtTwo	242.009	33.82	242.301	33.774	135	15
pine_extension_new	241.238	34.431	241.356	34.516	90	15
Pinto2	243.637	34.161	244	34.14	90	15
RaymondHill01a_newa	241.587	34.051	241.719	34.109	135	15
RaymondHill01a_newb	241.719	34.109	241.733	34.115	135	15
raymond_trace_02	242.011	34.163	242.015	34.161	90	15
raymond_trace_03	242	34.162	242.011	34.163	105	15
raymond_trace_06	241.965	34.15	242	34.162	105	15
raymond_trace_12	241.956	34.143	241.965	34.15	105	15
raymond_trace_14	241.951	34.142	241.956	34.143	105	15
raymond_trace_15	241.947	34.14	241.951	34.142	105	15
raymond_trace_16	241.944	34.141	241.947	34.14	105	15
raymond_trace_17	241.941	34.14	241.944	34.141	105	15
raymond_trace_18	241.917	34.13	241.941	34.14	105	15
raymond_trace_24	241.914	34.13	241.917	34.13	105	15
raymond_trace_25	241.894	34.125	241.914	34.13	105	15
raymond_trace_29	241.887	34.124	241.894	34.125	105	15
raymond_trace_31	241.883	34.122	241.887	34.124	105	15
raymond_trace_32	241.873	34.119	241.883	34.122	105	15
raymond_trace_36	241.87	34.118	241.873	34.119	105	15
raymond_trace_38	241.861	34.119	241.87	34.118	105	15
raymond_trace_40	241.842	34.119	241.861	34.119	105	15
raymond_trace_43	241.837	34.12	241.842	34.119	105	15
raymond_trace_44	241.834	34.119	241.837	34.12	105	15
raymond_trace_45	241.809	34.12	241.834	34.119	105	15
raymond_trace_50	241.777	34.122	241.809	34.12	105	15
raymond_trace_52	241.733	34.115	241.777	34.122	105	15
red_mountain_trace_26	240.576	34.358	240.617	34.341	120	15
red_mountain_trace_33	240.469	34.359	240.576	34.358	120	15
red_mountain_trace_38	240.447	34.353	240.469	34.359	120	15
red_mountain_trace_42	240.436	34.353	240.447	34.353	120	15
red_mountain_trace_44	240.432	34.352	240.436	34.353	120	15
red_mountain_trace_45	240.411	34.355	240.432	34.352	120	15
red_mountain_trace_48	240.407	34.355	240.411	34.355	120	15
red_mountain_trace_49	240.404	34.356	240.407	34.355	120	15
red_mountain_trace_50	240.379	34.36	240.404	34.356	120	15
red_mountain_trace_54	240.348	34.359	240.379	34.36	120	15
red_mountain_trace_59	240.342	34.36	240.348	34.359	120	15
red_mountain_trace_60	240.337	34.359	240.342	34.36	120	15
red_mountain_trace_61	240.293	34.365	240.337	34.359	120	15

Name	longitude1	latitude1	longitude2	latitude2	dip	locking depth
red_mountain_trace_68	240.284	34.365	240.293	34.365	120	15
red_mountain_trace_69	240.271	34.367	240.284	34.365	120	15
red_mountain_trace_71	240.254	34.363	240.271	34.367	120	15
red_mountain_trace_74	240.251	34.364	240.254	34.363	120	15
red_mountain_trace_75	240.247	34.364	240.251	34.364	120	15
red_mountain_trace_76	240.244	34.365	240.247	34.364	120	15
red_mountain_trace_77	240.242	34.367	240.244	34.365	120	15
red_mountain_trace_78	240.229	34.374	240.242	34.367	120	15
red_mountain_trace_80	240.213	34.375	240.229	34.374	120	15
red_mountain_trace_82	240.204	34.377	240.213	34.375	120	15
red_mountain_trace_84	240.199	34.377	240.204	34.377	120	15
red_mountain_trace_85	240.191	34.379	240.199	34.377	120	15
red_mountain_trace_86	240.179	34.378	240.191	34.379	120	15
red_mountain_trace_88	240.173	34.378	240.179	34.378	120	15
red_mountain_trace_91	240.126	34.388	240.173	34.378	120	15
red_mountain_trace_99	240.1	34.395	240.126	34.388	120	15
red_mountain_trace_103	240.094	34.396	240.1	34.395	120	15
red_mountain_trace_104	240.087	34.398	240.094	34.396	120	15
red_mountain_trace_105	240.061	34.401	240.087	34.398	120	15
red_mountain_trace_109	239.614	34.359	240.061	34.401	120	15
red_mountain_110	239.403	34.334	239.614	34.359	120	15
SAF_to_OV_closure1	191.871	57.592	216.76	55.69	90	15
SAF_to_PAC_southern_closure1	259.341	1.742	260.639	5.079	90	15
salinevalley1	241.946	37.15	242.048	36.925	90	10
sanandreas1ab	235.278	40.845	237.416	37.772	90	15
sanandreas1ba	237.416	37.772	239.157	36.265	90	0
sanandreas1bba	239.157	36.265	239.378	36.066	90	10
sanandreas1bbb	239.378	36.066	239.44	36.002	90	10
sa_parkfield_trace_01	239.44	36.002	239.707	35.749	90	15
sa_cholame_trace_02	239.707	35.749	240.137	35.311	90	15
sa_cholame_trace_01	240.137	35.311	240.14	35.307	90	15
carrizo_trace_05	240.14	35.307	240.361	35.114	90	15
carrizo_trace_04b	240.361	35.114	240.478	35.027	90	15
carrizo_trace_04a	240.478	35.027	240.594	34.94	90	15
carrizo_trace_03b	240.594	34.94	240.756	34.875	90	15
carrizo_trace_03a	240.756	34.875	240.79	34.864	90	15
carrizo_02	240.79	34.864	241.072	34.818	90	20
sanandreas8	241.072	34.818	241.548	34.677	90	25
sanandreas9	241.548	34.677	242.195	34.428	90	25
sanandreas10	242.195	34.428	242.453	34.318	90	25
sanandreas11	242.453	34.318	242.601	34.239	90	25
sanandreas12	242.601	34.239	242.663	34.207	90	15
sanandreas13	242.663	34.207	243.09	34.036	90	15
sanandreas19	243.09	34.036	243.141	33.997	90	25
sanandreas20	243.141	33.997	243.182	33.956	90	15
sanandreas21	243.182	33.956	243.215	33.946	90	15
sanandreas29	243.215	33.946	243.227	33.932	90	25
sanandreas30	243.227	33.932	243.252	33.927	90	25
sanandreas31	243.252	33.927	243.277	33.942	90	15
sanandreas32	243.277	33.942	243.301	33.942	90	15
sanandreas39	243.301	33.942	243.487	33.89	90	25

Name	longitude1	latitude1	longitude2	latitude2	dip	locking depth
sanandreas40	243.487	33.89	243.573	33.842	90	25
sanandreas41	243.573	33.842	243.589	33.843	90	25
sanandreas42	243.589	33.843	243.611	33.852	90	15
sanandreas43	243.611	33.852	243.681	33.818	90	25
sanandreas44a	243.681	33.818	243.76	33.775	90	10
sanandreas44b	243.76	33.775	243.814	33.747	90	10
sanandreas45	243.814	33.747	243.85	33.711	90	15
sanandreas46	243.85	33.711	244.239	33.391	90	15
sanandreas47	244.239	33.391	244.267	33.372	90	15
sanandreas48	244.267	33.372	244.293	33.347	90	15
sanandreas49	244.293	33.347	244.494	32.908	90	10
sanandreas50_newa	244.494	32.908	244.538	32.849	90	0
sanandreas50_newba	244.538	32.849	244.651	32.705	90	0
sanandreas50_newbb	244.651	32.705	245.066	32.154	90	0
sanandreas51	245.066	32.154	247.749	29.024	90	15
sanandreas52	247.749	29.024	260.639	5.079	90	15
sanjacinto_01	244.472	32.794	244.651	32.705	90	15
sanjacinto_02	244.302	32.886	244.472	32.794	90	15
sanjacinto_03	244.21	33.001	244.302	32.886	90	15
sanjacinto_04	243.901	33.258	244.21	33.001	90	15
sanjacinto_05	243.862	33.278	243.901	33.258	90	15
sanjacinto_06	243.853	33.287	243.862	33.278	90	15
sanjacinto_07	243.79	33.317	243.853	33.287	90	15
sanjacinto_08	243.789	33.323	243.79	33.317	90	15
sanjacinto_09	243.703	33.386	243.789	33.323	90	15
sanjacinto_10	243.607	33.418	243.703	33.386	90	15
sanjacinto_11	243.165	33.694	243.607	33.418	90	15
sanjacinto_12	243.104	33.743	243.165	33.694	90	15
sanjacinto_13	243.096	33.75	243.104	33.743	90	15
sanjacinto_14	243.073	33.791	243.096	33.75	90	15
sanjacinto_15	243.015	33.837	243.073	33.791	90	15
sanjacinto_16	242.988	33.847	243.015	33.837	90	15
sanjacinto_17	242.778	34.008	242.988	33.847	90	15
sanjacinto_18	242.746	34.029	242.778	34.008	90	15
sanjacinto_19	242.675	34.103	242.746	34.029	90	15
sanjacinto_20	242.671	34.112	242.675	34.103	90	15
sanjacinto_21	242.664	34.118	242.671	34.112	90	15
sanjacinto_22	242.651	34.138	242.664	34.118	90	15
sanjacinto_23	242.648	34.139	242.651	34.138	90	15
sanjacinto_24	242.636	34.161	242.648	34.139	90	15
sanjacinto_25	242.617	34.174	242.636	34.161	90	15
sanjacinto_26	242.605	34.178	242.617	34.174	90	15
san_cayetano_trace_01	241.228	34.423	241.238	34.431	135	15
san_cayetano_trace_04	241.215	34.42	241.228	34.423	135	15
san_cayetano_trace_07	241.207	34.422	241.215	34.42	135	15
san_cayetano_trace_10	241.197	34.422	241.207	34.422	135	15
san_cayetano_trace_11	241.191	34.417	241.197	34.422	135	15
san_cayetano_trace_13	241.172	34.409	241.191	34.417	135	15
san_cayetano_trace_18	241.161	34.4	241.172	34.409	135	15
san_cayetano_trace_21	241.14	34.395	241.161	34.4	135	15
san_cayetano_trace_29	241.125	34.395	241.14	34.395	135	15

Name	longitude1	latitude1	longitude2	latitude2	dip	locking depth
san_cayetano_trace_30	241.116	34.397	241.125	34.395	135	15
san_cayetano_trace_32	241.107	34.398	241.116	34.397	135	15
san_cayetano_trace_34	241.1	34.401	241.107	34.398	135	15
san_cayetano_trace_36	241.094	34.409	241.1	34.401	135	15
san_cayetano_trace_38	241.085	34.414	241.094	34.409	135	15
san_cayetano_trace_40	241.081	34.42	241.085	34.414	135	15
san_cayetano_trace_45	241.074	34.441	241.081	34.42	135	15
san_cayetano_trace_49	241.061	34.444	241.074	34.441	135	15
san_cayetano_trace_53	241.058	34.444	241.061	34.444	135	15
san_cayetano_trace_54	241.036	34.427	241.058	34.444	135	15
san_cayetano_trace_61	241.024	34.422	241.036	34.427	135	15
san_cayetano_trace_63	241.016	34.424	241.024	34.422	135	15
san_cayetano_trace_64	241.007	34.42	241.016	34.424	135	15
san_cayetano_trace_65	240.94	34.426	241.007	34.42	135	15
san_cayetano_trace_68	240.924	34.433	240.94	34.426	135	15
san_cayetano_trace_73	240.898	34.431	240.924	34.433	135	15
san_cayetano_trace_76	240.886	34.433	240.898	34.431	135	15
san_cayetano_trace_79	240.876	34.442	240.886	34.433	135	15
san_cayetano_trace_82	240.863	34.445	240.876	34.442	135	15
san_cayetano_trace_85	240.859	34.447	240.863	34.445	135	15
san_cayetano_trace_86	240.819	34.456	240.859	34.447	135	15
sancayetano_93	240.8	34.465	240.819	34.456	135	5
sancayetano_94	240.583	34.422	240.8	34.465	135	5
san_clemente_trace_01	242.609	31.997	242.615	31.995	90	15
san_clemente_trace_02	242.559	32.029	242.609	31.997	90	15
san_clemente_trace_08	242.549	32.039	242.559	32.029	90	15
san_clemente_trace_10	242.495	32.063	242.549	32.039	90	15
san_clemente_trace_15	242.447	32.1	242.495	32.063	90	15
san_clemente_trace_20	242.444	32.109	242.447	32.1	90	15
san_clemente_trace_21	242.393	32.126	242.444	32.109	90	15
san_clemente_trace_26	242.356	32.153	242.393	32.126	90	15
san_clemente_trace_29	242.342	32.171	242.356	32.153	90	15
san_clemente_trace_31	242.332	32.174	242.342	32.171	90	15
san_clemente_trace_32	242.307	32.206	242.332	32.174	90	15
san_clemente_trace_35	242.084	32.395	242.307	32.206	90	15
san_clemente_trace_64	242.001	32.545	242.084	32.395	90	15
san_clemente_trace_81	241.944	32.597	242.001	32.545	90	15
san_clemente_trace_88	241.918	32.643	241.944	32.597	90	15
san_clemente_trace_94	241.832	32.704	241.918	32.643	90	15
san_clemente_trace_107	241.805	32.713	241.832	32.704	90	15
san_clemente_trace_110	241.668	32.838	241.805	32.713	90	15
san_clemente_trace_130	241.634	32.891	241.668	32.838	90	15
san_clemente_trace_135	241.602	32.918	241.634	32.891	90	15
san_clemente_trace_138	241.557	32.938	241.602	32.918	90	15
san_clemente_trace_143	241.535	32.956	241.557	32.938	90	15
san_clemente_trace_145	241.479	33.033	241.535	32.956	90	15
san_clemente_trace_151	241.218	33.273	241.479	33.033	90	15
san_clemente_trace_172	241.192	33.288	241.218	33.273	90	15
san_gabriel_00	242.369	34.265	242.453	34.318	90	15
san_gabriel_trace_01	242.341	34.243	242.369	34.265	90	15
san_gabriel_trace_02	242.32	34.237	242.341	34.243	90	15

Name	longitude1	latitude1	longitude2	latitude2	dip	locking depth
san_gabriel_trace_03	242.257	34.245	242.32	34.237	90	15
san_gabriel_trace_04	242.217	34.244	242.257	34.245	90	15
san_gabriel_trace_05	242.144	34.253	242.217	34.244	90	15
san_gabriel_trace_06	242.111	34.259	242.144	34.253	90	15
san_gabriel_trace_07	242.061	34.251	242.111	34.259	90	15
san_gabriel_trace_08	242.007	34.251	242.061	34.251	90	15
san_gabriel_trace_09	241.965	34.248	242.007	34.251	90	15
san_gabriel_trace_10	241.912	34.255	241.965	34.248	90	15
san_gabriel_trace_11	241.868	34.283	241.912	34.255	90	15
san_gabriel_trace_12	241.826	34.296	241.868	34.283	90	15
san_gabriel_trace_13	241.745	34.303	241.826	34.296	90	15
san_gabriel_trace_16	241.716	34.321	241.745	34.303	90	15
san_gabriel_trace_17	241.699	34.333	241.716	34.321	90	15
san_gabriel_trace_18	241.675	34.343	241.699	34.333	90	15
san_gabriel_trace_19	241.643	34.35	241.675	34.343	90	15
san_gabriel_trace_20	241.599	34.365	241.643	34.35	90	15
san_gabriel_trace_21	241.572	34.372	241.599	34.365	130	15
san_gabriel_trace_22	241.489	34.408	241.572	34.372	130	15
san_gabriel_trace_24	241.405	34.459	241.489	34.408	130	15
san_gabriel_trace_26	241.356	34.516	241.405	34.459	130	15
san_gabriel_trace_28	241.333	34.533	241.356	34.516	130	15
san_gabriel_trace_29	241.271	34.584	241.333	34.533	130	15
san_gabriel_trace_31	241.149	34.7	241.271	34.584	130	15
san_gabriel_trace_35	241.125	34.716	241.149	34.7	130	15
sangabriel2aa_new	241.072	34.818	241.125	34.716	130	15
san_gregorio1	237.416	37.772	238.131	36.359	90	15
santa_cruz_monica_connect	240.74	33.984	240.767	34.029	90	15
santamonicamtns3	241.034	34.028	241.36	34.014	135	15
santamonicamtns4	241.36	34.014	241.498	34.023	135	15
santamonicamtns5a	241.498	34.023	241.587	34.051	135	15
BradsNewSantaMonica01a	240.661	34.237	240.767	34.029	135	15
BradsNewSantaMonica01b	240.767	34.029	241.034	34.028	135	15
santarosa_channel_connect	239.889	33.973	240.089	33.903	90	15
santa_rosa_island_trace_04	239.82	33.974	239.889	33.973	90	15
santa_rosa_island_trace_05	239.77	33.985	239.82	33.974	90	15
santa_rosa_island_trace_06	239.642	33.989	239.77	33.985	90	15
santa_rosa_island_trace_08	239.57	33.989	239.642	33.989	90	15
santa_rosa_island_trace_09	239.489	34.022	239.57	33.989	90	15
santa_susana_connect	241.651	34.311	241.656	34.316	135	15
santa_susana_trace_02	241.626	34.32	241.651	34.311	135	15
santa_susana_trace_10	241.62	34.32	241.626	34.32	135	15
santa_susana_trace_12	241.603	34.326	241.62	34.32	135	15
santa_susana_trace_17	241.597	34.33	241.603	34.326	135	15
santa_susana_trace_19	241.594	34.328	241.597	34.33	135	15
santa_susana_trace_20	241.571	34.33	241.594	34.328	135	15
santa_susana_trace_25	241.568	34.328	241.571	34.33	135	15
santa_susana_trace_26	241.54	34.327	241.568	34.328	135	15
santa_susana_trace_32	241.534	34.33	241.54	34.327	135	15
santa_susana_trace_34	241.508	34.327	241.534	34.33	135	15
santa_susana_trace_40	241.491	34.313	241.508	34.327	135	15
santa_susana_trace_46	241.486	34.311	241.491	34.313	135	15

Name	longitude1	latitude1	longitude2	latitude2	dip	locking depth
santa_susana_trace_48	241.483	34.306	241.486	34.311	135	15
santa_susana_trace_50	241.453	34.302	241.483	34.306	135	15
santa_susana_trace_58	241.421	34.305	241.453	34.302	135	15
santa_susana_trace_66	241.419	34.311	241.421	34.305	135	15
santa_susana_trace_68	241.415	34.312	241.419	34.311	135	15
santa_susana_trace_69	241.41	34.306	241.415	34.312	135	15
santa_susana_trace_71	241.407	34.307	241.41	34.306	135	15
santa_susana_trace_72	241.407	34.307	241.407	34.321	90	15
santa_susana_trace_76	241.4	34.319	241.407	34.321	135	15
santa_susana_trace_78	241.4	34.319	241.402	34.314	135	15
santa_susana_trace_79	241.393	34.309	241.402	34.314	135	15
santa_susana_trace_82	241.388	34.31	241.393	34.309	135	15
santa_susana_trace_83	241.387	34.316	241.388	34.31	135	15
santa_susana_trace_85	241.382	34.318	241.387	34.316	135	15
santa_susana_trace_87	241.38	34.324	241.382	34.318	135	15
santa_susana_trace_89	241.38	34.324	241.384	34.324	90	15
santa_susana_trace_90	241.384	34.324	241.385	34.327	90	15
santa_susana_trace_91	241.379	34.331	241.385	34.327	135	15
santa_susana_trace_93	241.371	34.331	241.379	34.331	135	15
santa_susana_trace_95	241.367	34.338	241.371	34.331	135	15
santa_susana_trace_97	241.359	34.334	241.367	34.338	135	15
santa_susana_trace_100	241.355	34.334	241.359	34.334	135	15
santa_susana_trace_101	241.355	34.334	241.357	34.341	90	15
santa_susana_trace_103	241.351	34.34	241.357	34.341	135	15
santa_susana_trace_105	241.339	34.347	241.351	34.34	135	15
santa_susana_trace_109	241.331	34.353	241.339	34.347	135	15
santa_susana_trace_112	241.319	34.355	241.331	34.353	135	15
santa_susana_trace_116	241.317	34.353	241.319	34.355	135	15
santa_susana_trace_117	241.311	34.351	241.317	34.353	135	15
santa_susana_trace_119	241.308	34.346	241.311	34.351	135	15
santa_susana_trace_121	241.303	34.344	241.308	34.346	135	15
santa_susana_trace_123	241.298	34.347	241.303	34.344	135	15
santa_susana_trace_125	241.294	34.343	241.298	34.347	135	15
santa_susana_trace_127	241.277	34.345	241.294	34.343	135	15
santa_susana_trace_131	241.272	34.348	241.277	34.345	135	15
santa_susana_trace_133	241.267	34.344	241.272	34.348	135	15
santa_susana_trace_135	241.266	34.347	241.267	34.344	135	15
santa_susana_trace_136	241.262	34.349	241.266	34.347	135	15
santa_susana_trace_137	241.26	34.352	241.262	34.349	135	15
santa_susana_trace_138	241.254	34.354	241.26	34.352	135	15
santa_susana_trace_140	241.249	34.359	241.254	34.354	135	15
santa_susana_trace_142	241.246	34.357	241.249	34.359	135	15
santa_susana_trace_143	241.242	34.361	241.246	34.357	135	15
santa_susana_trace_145	241.241	34.365	241.242	34.361	135	15
santa_susana_trace_146	241.238	34.368	241.241	34.365	135	15
santa_susana_trace_147	241.233	34.367	241.238	34.368	135	15
santa_susana_trace_148	241.229	34.372	241.233	34.367	135	15
sierramadre_00	242.119	34.147	242.272	34.125	130	15
sierra_madre_trace_02	242.06	34.15	242.119	34.147	130	15
sierra_madre_trace_03	242.015	34.161	242.06	34.15	130	15
sierra_madre_trace_04	241.997	34.175	242.015	34.161	130	15

Name	longitude1	latitude1	longitude2	latitude2	dip	locking depth
sierra_madre_trace_05	241.932	34.176	241.997	34.175	130	15
sierra_madre_trace_06	241.888	34.201	241.932	34.176	130	15
sierra_madre_trace_07	241.851	34.203	241.888	34.201	130	15
sierra_madre_trace_08	241.786	34.213	241.851	34.203	130	15
sierra_madre_trace_09	241.754	34.228	241.786	34.213	130	15
sierra_madre_trace_10	241.72	34.258	241.754	34.228	130	15
sierra_madre_trace_11	241.71	34.275	241.72	34.258	130	15
sierra_madre_trace_12	241.702	34.284	241.71	34.275	130	15
sierra_madre_trace_13	241.694	34.284	241.702	34.284	130	15
sierramadre_sangabriel_connecta	241.656	34.316	241.694	34.284	130	15
sierramadre_sangabriel_connectb	241.599	34.365	241.656	34.316	130	15
sierra_nevada_00	241.977	35.296	241.978	35.285	90	15
sierra_nevada_trace_01	241.97	35.306	241.977	35.296	90	15
sierra_nevada_trace_02	241.967	35.32	241.97	35.306	90	15
sierra_nevada_trace_03	241.965	35.338	241.967	35.32	90	15
sierra_nevada_trace_04	241.96	35.349	241.965	35.338	90	15
sierra_nevada_trace_05	241.955	35.379	241.96	35.349	90	15
sierra_nevada_trace_06	241.949	35.428	241.955	35.379	90	15
sierra_nevada_trace_07	241.949	35.428	241.952	35.443	90	15
sierra_nevada_trace_08	241.952	35.443	241.953	35.451	90	15
sierra_nevada_trace_09	241.953	35.451	241.953	35.468	90	15
sierra_nevada_trace_10	241.953	35.468	241.953	35.483	90	15
sierra_nevada_trace_11	241.953	35.483	241.956	35.498	90	15
sierra_nevada_trace_12	241.956	35.498	241.958	35.52	90	15
sierra_nevada_trace_13	241.958	35.52	241.962	35.527	90	15
sierra_nevada_trace_14	241.962	35.527	241.964	35.535	90	15
sierra_nevada_trace_15	241.964	35.535	241.966	35.54	90	15
sierra_nevada_trace_16	241.966	35.54	241.971	35.548	90	15
sierra_nevada_trace_17	241.971	35.548	241.983	35.56	90	15
sierra_nevada_trace_18	241.983	35.56	241.996	35.57	90	15
sierra_nevada_trace_19	241.996	35.57	242.035	35.578	90	15
sierra_nevada_trace_21	242.035	35.578	242.091	35.612	90	15
sierra_nevada_trace_27	242.091	35.612	242.123	35.657	90	15
sierra_nevada_trace_30	242.123	35.657	242.131	35.686	90	15
sierra_nevada_trace_33	242.112	35.734	242.131	35.686	90	15
sierra_nevada_trace_36	242.096	35.761	242.112	35.734	90	15
sierra_nevada_trace_38	242.096	35.761	242.105	35.88	90	15
sierra_nevada_trace_42	242.065	35.949	242.105	35.88	90	15
sierra_nevada_trace_43	242.046	35.973	242.065	35.949	90	15
sierra_nevada_trace_45	242.017	36.055	242.046	35.973	90	15
sierra_nevada_trace_48	242.015	36.082	242.017	36.055	90	15
sierra_nevada_trace_50	241.996	36.105	242.015	36.082	90	15
sierra_nevada_trace_51	241.991	36.126	241.996	36.105	90	15
sierra_nevada_trace_52	241.991	36.126	242.008	36.155	90	15
sierra_nevada_trace_54	242.007	36.178	242.008	36.155	90	15
sierra_nevada_trace_55	242.007	36.178	242.014	36.192	90	15
sierra_nevada_trace_56	242.014	36.192	242.015	36.2	90	15
sierra_nevada_trace_57	241.988	36.269	242.015	36.2	90	15
sierra_nevada_trace_62	241.96	36.295	241.988	36.269	90	15
sierra_nevada_trace_63	241.96	36.295	241.977	36.35	90	15
sierra_nevada_trace_69	241.967	36.41	241.977	36.35	90	15

Name	longitude1	latitude1	longitude2	latitude2	dip	locking depth
sierranevada_73	241.967	36.41	241.98	36.507	90	15
Western_closure01	204.097	-69.387	252.514	-42.884	90	15
Western_closure02	162.871	-57.774	180.29	-36.871	90	15
Western_closure03	162.871	-57.774	204.097	-69.387	90	15
Western_closure04	252.514	-42.884	259.341	1.742	90	15
Western_closure05	145.025	41.058	162.912	55.592	90	15
Western_closure06	142.758	34.025	145.025	41.058	90	15
Western_closure07	131.169	29.806	142.758	34.025	90	15
Western_closure08	124.115	3.316	131.169	29.806	90	15
Western_closure09	124.115	3.316	164.764	-7.061	90	15
Western_closure10	164.764	-7.061	180.29	-36.871	90	15
Western_closure11	162.912	55.592	190.538	57.203	90	15
westnorthfrontalzone01	242.663	34.207	242.773	34.345	45	15
westnorthfrontalzone02	242.773	34.345	242.776	34.371	45	15
westnorthfrontalzone03	242.776	34.371	242.799	34.369	45	15
westnorthfrontalzone05	242.799	34.369	242.799	34.405	45	15
westnorthfrontalzone06	242.799	34.405	242.833	34.439	45	15
westnorthfrontalzone07	242.833	34.439	242.855	34.444	45	15
westnorthfrontalzone08	242.855	34.444	242.892	34.441	45	15
westnorthfrontalzone09	242.892	34.441	242.997	34.396	45	15
westnorthfrontalzone10	242.997	34.396	243.011	34.382	45	15
westnorthfrontalzone11	243.011	34.382	243.062	34.365	45	15
westnorthfrontalzone12	243.062	34.365	243.148	34.371	45	15
white_wolf_trace_01	241.462	35.322	241.525	35.385	45	15
white_wolf_trace_04	241.452	35.321	241.462	35.322	45	15
white_wolf_trace_05	241.414	35.293	241.452	35.321	45	15
white_wolf_trace_09	241.413	35.287	241.414	35.293	45	15
white_wolf_trace_11	241.41	35.282	241.413	35.287	45	15
white_wolf_trace_12	241.403	35.276	241.41	35.282	45	15
white_wolf_trace_13	241.398	35.269	241.403	35.276	45	15
white_wolf_trace_15	241.388	35.264	241.398	35.269	45	15
white_wolf_trace_16	241.375	35.265	241.388	35.264	45	15
white_wolf_trace_17	241.356	35.256	241.375	35.265	45	15
white_wolf_trace_18	241.341	35.246	241.356	35.256	45	15
white_wolf_trace_19	241.328	35.234	241.341	35.246	45	15
white_wolf_trace_20	241.298	35.22	241.328	35.234	45	15
white_wolf_trace_22	241.285	35.211	241.298	35.22	45	15
white_wolf_trace_23	241.275	35.208	241.285	35.211	45	15
white_wolf_trace_24	241.265	35.212	241.275	35.208	45	15
white_wolf_trace_25	241.258	35.209	241.265	35.212	45	15
white_wolf_trace_26	241.25	35.201	241.258	35.209	45	15
white_wolf_trace_27	241.221	35.179	241.25	35.201	45	15
white_wolf_trace_28	241.214	35.17	241.221	35.179	45	15
white_wolf_trace_29	241.189	35.148	241.214	35.17	45	15
white_wolf_trace_31	241.172	35.138	241.189	35.148	45	15
white_wolf_trace_32	241.159	35.126	241.172	35.138	45	15
white_wolf_trace_33	240.926	34.992	241.159	35.126	45	15
white_wolf_35	240.756	34.875	240.926	34.992	45	15
white_wolf_36	241.525	35.385	242.105	35.88	45	15